

# Silicon and Nickel Enrichment in Planet-Host Stars: Observations and Implications for the Core-Accretion Theory of Planet Formation

Sarah E. Robinson<sup>1</sup>, Gregory Laughlin<sup>1</sup>, Peter Bodenheimer<sup>1</sup>, and Debra Fischer<sup>2</sup>

## ABSTRACT

We present evidence that stars with planets exhibit statistically significant silicon and nickel enrichment over the general metal-rich population. We also present simulations which predict silicon enhancement of planet hosts within the context of the core-accretion hypothesis for giant planet formation. Because silicon and oxygen are both  $\alpha$ -elements,  $[\text{Si}/\text{Fe}]$  traces  $[\text{O}/\text{Fe}]$ , so the silicon enhancement in planet hosts predicts that these stars are oxygen-rich as well. We present new numerical simulations of planet formation by core accretion that establish the timescale on which a Jovian planet reaches rapid gas accretion,  $t_{\text{rga}}$ , as a function of solid surface density  $\sigma_{\text{solid}}$ :  $(t_{\text{rga}}/1 \text{ Myr}) = (\sigma_{\text{solid}}/25.0 \text{ g cm}^{-2})^{-1.44}$ . This relation enables us to construct Monte Carlo simulations that predict the fraction of star-disk systems that form planets as a function of  $[\text{Fe}/\text{H}]$ ,  $[\text{Si}/\text{Fe}]$ , disk mass, outer disk radius and disk lifetime. Our simulations reproduce both the known planet-metallicity correlation and the planet-silicon correlation reported in this paper. The simulations predict that 16% of Solar-type stars form Jupiter-mass planets, in agreement with 12% predicted from extrapolation of the observed planet frequency-semimajor axis distribution. Although a simple interpretation of core accretion predicts that the planet-silicon correlation should be much stronger than the planet-nickel correlation, we observe the same degree of silicon and nickel enhancement in planet hosts. If this result persists once more planets have been discovered, it might indicate a complexity in the chemistry of planet formation beyond the simple accumulation of solids in the core accretion theory.

*Subject headings:* planetary systems — stars: abundances, solar system: formation, methods: statistical

---

<sup>1</sup>University of California Observatories/Lick Observatory, Department of Astronomy and Astrophysics, University of California at Santa Cruz, Interdisciplinary Sciences Building, Santa Cruz, CA 95064; ser@ucolick.org, laughlin@ucolick.org, peter@ucolick.org

<sup>2</sup>Department of Physics & Astronomy, San Francisco State University, San Francisco, CA 94132; fisher@stars.sfsu.edu

## 1. Introduction

Since the first recognition that metal-rich stars are more likely to harbor planets (Gonzalez 1997), there have been tantalizing suggestions that planet hosts undergo a different process of chemical development than planetless field stars. Gonzalez (1997) proposed that stars with planets are metal-rich because they self-pollute by planetesimal accretion during the planet-formation epoch. Sandquist et al. (1998) found that accretion of a few tens of earth masses of planetesimals would account for all the metals present in the convective envelope of solar-type stars, but the giant-planet migration mechanism for scattering such a substantial planetesimal mass into the host star is only possible if 90% of close encounters result in the outward ejection of planetesimals. Murray & Chaboyer (2002) confirmed that stars with planets are iron-rich, and proposed that accretion of  $5M_{\oplus}$  of iron, in addition to high primordial metallicity, would explain the trend. The self-pollution scenario leads to the expectation that planet hosts, although being iron-rich, have reduced abundances of volatiles such as C, N and O, because these would be minimally present in the accreted planetesimals (Smith et al. 2001). Finding no evidence of volatile depletion among stars with planets (Ecuivillon et al. 2004, Takeda & Honda 2005), most investigators have concluded that the iron enrichment of planet hosts is primordial: stars hosting giant planets form preferentially in metal-rich molecular clouds. This assessment concurs with the finding of Fischer & Valenti (2005) that there is no relation between metallicities of planet hosts and convection zone depth, either while the star is on the main sequence or after it evolves to the subgiant branch and its convection zone deepens. If pollution of stars by planetesimal accretion were responsible for the planet-metallicity correlation, planet hosts with the most shallow convection zones would have the highest metallicity (Laughlin & Adams 1997).

Barring planet host self-pollution as the chief cause of the planet-metallicity correlation, there is still the possibility that stars with planets form from molecular clouds with anomalous metal enrichment histories. Timmes, Woosley & Weaver (1995) calculated the enrichment pattern over time of metals from Li to Zn in sequences  $[X/Fe]$  vs.  $[Fe/H]$ . For most elements, these theoretical sequences closely match observations. If planet hosts do not lie on the same  $[X/Fe]$  vs.  $[Fe/H]$  sequences of chemical evolution as other Pop I stars, the enhanced iron abundance seen in planet hosts could be an artifact of this unusual chemical evolution. If the ability to form planets were uniformly the result of a particular type of chemical event—a nearby supernova, for example—planet hosts would show markedly different abundance distributions than field stars in both volatile and refractory elements. Yet analysis of the trends in  $[X/Fe]$  vs.  $[Fe/H]$  for  $\alpha$ - and Fe-peak elements by Bodaghee et al. (2003) reveals that abundance distributions of planet hosts are the high-metallicity extensions of the trends governing chemical evolution in planetless stars. A similar analysis by Huang et al. (2005) suggests that, although S & Mg may be enhanced in planet hosts (contrary to Ecuivillon et

al. 2004, who found no evidence of sulfur enhancement), they still follow the same slope in the  $[S/H]$  vs.  $[Fe/H]$  relation as the comparison sample of planetless field stars. We are left, then, with the conclusion that planet-bearing stars are indistinguishable from other Population I stars in their chemical enrichment histories, implying that no extraordinary chemical events are necessary to stimulate planet formation.

Working with the assumption that planet hosts belong to the same stellar population as other metal-rich field stars, is it still worth checking for patterns in the abundances of stars with planets? The studies mentioned above use comparison samples of planetless field stars with markedly lower median  $[Fe/H]$  than that of the planet hosts. Bodaghee et al. (2003) and Ecuivillon et al. (2004) have no stars in their comparison sample in the range  $0.2 \leq [Fe/H] \leq 0.5$ , which is where more than 1/3 of their planet hosts are found. Using a comparison sample with no stars of  $[Fe/H] \geq 0.1$ , Huang et al. (2005) could not tell if the Mg and S enhancement in their planet hosts was particular to stars with planets, or a characteristic of metal-rich stars in general. While comparison samples of this type allow the investigator to comment on the general chemical evolution trends of planet hosts, they cannot elucidate whether planet hosts systematically possess more or less of a certain element than field stars *of the same metallicity*. Comparison between planet hosts and field stars of the same metallicity probes a third type of relationship between element abundances and the presence or absence of planets: stars with planets do not self-enrich at birth, are not born in molecular clouds with chemically tumultuous histories; but they nevertheless may be enhanced or deficient in some element that aids the formation of planets, *simply due to the natural Galactic variation in stellar abundances*.

The chemical compositions of metal-rich stars are strikingly uniform: in the sample of metal-rich stars observed by Valenti & Fischer (2005),  $[X/Fe]$  at a given value of  $[Fe/H]$ , where  $X = Na, Si, Ti$  and  $Ni$ , is observed to vary by 0.4 dex at the very most (Valenti & Fischer 2005). However, Fischer & Valenti (2005), in their study of the planet-metallicity correlation, find that the probability of planet detection increases by a factor of five if when iron abundance is enhanced by a factor of two (0.3 dex). If a correlation of this magnitude exists between planet detectability and another element besides iron—or if iron abundance derives its power as a predictor of planet presence from its correlation with the abundance of another element of more physical importance to the planet-formation process—it will be detectable in the 0.4 dex spread of  $[X/Fe]$  in stars with the same value of  $[Fe/H]$ .

In this work, we present our statistical method for assessing the relationship between planet presence and the observed abundances of individual refractory elements. As specific examples of the method, in §2, we present statistical evidence of possible silicon and nickel enhancement in planet hosts, and we show additionally that titanium abundances display no

such correlation. In §3, we empirically determine the exponent of a power law giving probability of planet formation as a function of  $[\text{Si}/\text{Fe}]$ , among stars of the same  $[\text{Fe}/\text{H}]$ . Finally, in §4, we construct a simulation based on the core accretion theory that reproduces both the planet-metallicity correlation and our observed correlation between silicon abundance and presence of planets.

## 2. Observational Evidence for Silicon and Nickel Enhancement of Planet Hosts

The Spectroscopic Properties of Cool Stars catalog (Valenti & Fischer 2005, hereafter SPOCS) is a collection of stellar parameters for 1040 nearby FGK dwarfs, including 99 planet hosts<sup>1</sup>, that were observed as part of the Keck, Lick and AAT planet-search programs. The SPOCS data are uniform, since all observations were obtained by the same observers and analyzed with the same spectral-synthesis pipeline. SPOCS report abundances of five elements: sodium, the Fe-peak elements iron and nickel, and  $\alpha$ -process elements silicon and titanium, which were measured with high precision:  $\sigma_{[\text{Na}/\text{H}]} = 0.032$  dex,  $\sigma_{[\text{Fe}/\text{H}]} = 0.030$  dex,  $\sigma_{[\text{Si}/\text{H}]} = 0.019$  dex,  $\sigma_{[\text{Ti}/\text{H}]} = 0.046$  dex, and  $\sigma_{[\text{Ni}/\text{H}]} = 0.030$  dex. The low spread in element abundances at a given value of  $[\text{Fe}/\text{H}]$  means precision is paramount in any successful study of the chemistry of planet hosts. Because of the low random errors and uniformity of the metal abundances presented in the SPOCS catalog, it is an ideal arena in which to study differential abundances in planet-bearing stars.

Figure 1 shows plots of  $[\text{Si}/\text{Fe}]$ ,  $[\text{Ti}/\text{Fe}]$  and  $[\text{Ni}/\text{Fe}]$  as a function of  $[\text{Fe}/\text{H}]$  for the 1040 stars in the SPOCS compilation. In Figure 1, it appears that there is a difference in the silicon-to-iron ratio of planet hosts compared to the rest of the SPOCS stars: Planet hosts seem to concentrate in the silicon-rich part of the  $[\text{Si}/\text{Fe}]$ - $[\text{Fe}/\text{H}]$  locus. Similarly, the lack of planet hosts in the nickel-poor parts of the  $[\text{Ni}/\text{Fe}]$ - $[\text{Fe}/\text{H}]$  locus suggests that planet hosts might be nickel-enhanced as well. Our hypothesis, therefore, is that stars with planets have higher silicon-to-iron and nickel-to-iron ratios than are typical of the field star population. We also investigate a possible relationship between planet detection and  $[\text{Ti}/\text{Fe}]$ , even though no such trend is obvious in Figure 1. Our aim is to assess whether the visual evidence of Figure 1 corresponds to statistically significant silicon and nickel enhancement among planet hosts, and whether titanium abundance follows a similar trend, despite the lack of an immediate visual relationship.

---

<sup>1</sup>Valenti & Fischer observed Vesta to obtain a Solar spectrum, so we count the Sun as a planet host present in the SPOCS data.

To test our hypothesis, we would like to measure the likelihood that planet-host stars follow the same underlying  $[X/Fe]$  distribution as the field-star population, where  $X = Si, Ni$  and  $Ti$ . However, for any  $X$ ,  $[X/Fe]$  varies with  $[Fe/H]$ , reflecting the history of Galactic chemical evolution (Timmes, Woosley & Weaver 1995). Merely due to the planet-metallicity correlation, planet hosts will assuredly follow a different silicon or nickel abundance distribution than the field-star population, as reflected in Figure 1 of Bodaghee et al. (2003). If element  $X$  is intrinsically important to the process of planet formation, either as a building-block of giant planets, or as a tracer of some other fundamental process, the stars with the highest value of  $[X/Fe]$  *at a given iron abundance* will be the most likely to harbor planets. We will use a Kolmogorov-Smirnov (K-S) test (see, e.g. Press et al. 1992) to estimate the probability  $k$  that a synthetic set of stars with planets,  $B$ , follows the same  $[Si/Fe]$ ,  $[Ni/Fe]$  and  $[Ti/Fe]$  distributions as a control sample,  $C$ , of field stars, *if both samples are drawn from the same iron abundance distribution*. By matching the  $[Fe/H]$  distributions of  $B$  and  $C$ , we can control for the effects of Galactic chemical evolution, ensuring that we investigate only abundance patterns that correlate directly with the presence or absence of giant planets.

At this point, we make no assumptions about the physical processes by which planet formation might be stimulated by silicon or nickel enrichment of the host star, nor the distributions of the variables that control these processes (see §4 for a simulation of the relationship between  $[Si/Fe]$  and planet detection). We therefore choose a bootstrap Monte Carlo method, drawing from the SPOCS data with replacement to find  $B$  and  $C$ . We perform 100,000 bootstrap experiments to simulate the distribution  $D_X$  of Kolmogorov-Smirnov probabilities that would be expected from bootstrap realizations of a true probability  $\mathcal{P}_X$ , that the Galaxy’s planet hosts and field stars follow the same  $[X/Fe]$  distribution. The bootstrap method will only tell us the form and spread of  $D_X$ —it cannot determine the median around which  $D_X$  would be distributed in the limit  $k \rightarrow \mathcal{P}_X$ . If the abundance of  $X$  is correlated with probability of planet detection, the probability  $k$  returned by the K-S test should be low—but how low does it have to be to indicate a statistically significant effect? To answer this question, we need to test what  $D_X$  would look like if  $k$  were always calculated using two samples identically distributed in  $[X/Fe]$ .

Since we must control for the effects of Galactic chemical evolution, we always calculate realizations of  $k$  using samples of planet hosts and field stars selected from the same  $[Fe/H]$  distribution. We can find the K-S probability  $q$  that planet hosts of set  $B$  and field stars of set  $C$  follow the same distribution in  $[Fe/H]$ : By construction, the underlying distribution  $\mathcal{Q}$  of  $q$  is unity. In practice,  $q$  can never reach unity because of the impossibility of selecting different two sets of stars with  $[Fe/H]$  distributions that exactly match from a parent set of finite size.  $q > 0.5$  is consistent with the hypothesis that  $B$  and  $C$  truly have matching  $[Fe/H]$  distributions. The simulated distribution of  $q$ ,  $D_{Fe}$ , can be used as a benchmark to

assess  $D_X$ . We estimate  $\mathcal{P}_X$ , the true probability that planet hosts in the SPOCS data follow the same  $[X/Fe]$  distribution as other field stars of the same metallicity, by the following formula:

$$\mathcal{P}_S = \frac{\int_0^1 D_X D_{Fe} p dp}{\int_0^1 D_{Fe}^2 p dp}, \quad (1)$$

where  $p$  denotes probability. See Appendix A for a detailed description of the statistical methods used to find  $D_X$  and  $D_{Fe}$ .

Figure 2 shows the result of the Monte Carlo simulations. For silicon, we find a probability  $\mathcal{P}_{Si}$  that planet hosts and field stars are drawn from the same  $[Si/Fe]$  distribution of 0.23. In addition,  $D_{Si}$  clearly has a different form than  $D_{Fe}$ . Forcing the control set to follow the planet hosts’ metallicity distribution succeeds in almost all simulations: The median of  $D_{Fe}$  is 0.61 and  $D_{Fe}$  falls as  $q \rightarrow 0$ . However,  $D_{Si}$  has median 0.079, and declines rapidly as  $p \rightarrow 1$ . The results shown in Figure 2 indicate that even when the effects of Galactic chemical evolution are taken into account, stars with planets do not have the same silicon abundance distribution as the general field star population. There is, therefore, evidence that, at a given iron abundance, a star’s probability of harboring a detectable planet depends on its silicon abundance.

For nickel, we find  $\mathcal{P}_{Ni} = 0.25$ , and  $D_{Ni}$ , like  $D_{Si}$ , is skewed toward low probabilities that the planet hosts and field stars have matching  $[Ni/Fe]$  distributions. There is then evidence that, at a given  $[Fe/H]$ , a star’s probability of harboring a detectable planet depends on its nickel abundance. For titanium, we find  $\mathcal{P}_{Ti} = 0.78$ , and  $D_{Ti}$  appears to have a similar form to  $D_{Fe}$ . There is, therefore, no statistical evidence that titanium abundance is correlated with planet detection probability, other than as an overall metallicity indicator.

We still have not given direct evidence for our original hypothesis, that planets are more likely to be detected around silicon-rich and nickel-rich, than silicon-poor and nickel-poor stars—we have merely shown that the silicon abundances of planet hosts are systematically *different* from those of the field-star population. In Figure 1, it looks like stars with planets might be more likely to be silicon- and nickel-enhanced. This impression is confirmed by Figure 3, where we have binned the SPOCS data by iron metallicity and plotted the percent of stars with planets as a function of  $[Si/Fe]$  and  $[Ni/Fe]$ . Two things are apparent in Figure 3: (1) the stars with planets are to be found at the top of the range of silicon or nickel abundances exhibited by the stars in each bin; and (2) the general trend is that the fraction of stars with planets rises toward higher silicon or nickel abundance. The exception to (2) is the bin  $0.35 < [Fe/H] < 0.45$  dex—there are only 33 stars in this bin (as opposed to more than 100 in each of the other bins), so it may suffer from small-sample statistics.

We note that accurate calculation of  $\mathcal{P}_{Ni}$  and  $\mathcal{P}_{Si}$  depends on the stars in SPOCS having

been selected for the Keck planet-search program without any reference to silicon or nickel content. One of program’s aims was to obtain high-resolution spectra of as many planet hosts as possible, so the host stars of planets discovered by other groups were added to the survey. This definitely introduces a bias in the planet hosts’ [Fe/H] distribution, which we have corrected by comparing the planet hosts with control samples that have the same [Fe/H] distribution. If, as our analysis suggests, planet hosts are more likely to be silicon- or nickel-enhanced than field stars of the same metallicity, adding planet hosts discovered by other groups to the SPOCS survey would amplify any existing correlation between presence of planets and [Si/Fe] or [Ni/Fe].

Recognizing that observing planet hosts discovered by other groups would bias the [Fe/H] distribution of SPOCS, Fischer & Valenti (2005) identified a set of stars with uniform planet detectability, requiring that all stars in this set be independently selected targets for the Keck, Lick and AAT planet searches, and have at least 10 observations spanning four years with  $30 \text{ m s}^{-1}$  or better radial-velocity precision. This uniform set, which contains 850 stars and 47 planet hosts, was used to study the planet-metallicity correlation. To confirm that the suggestion of silicon and nickel enhancement among planet hosts is not the result of SPOCS selection biases, we perform our statistical analysis of the [Si/Fe], [Ni/Fe] and [Ti/Fe] distributions of planet hosts on the uniform set, using 10,000 bootstrap Monte Carlo simulations. We find  $\mathcal{P}_{\text{Si}} = 0.20$ ,  $\mathcal{P}_{\text{Ni}} = 0.25$ , and  $\mathcal{P}_{\text{Ti}} = 0.94$ . The value of  $\mathcal{P}_{\text{Si}}$  is slightly lower using the uniform data set than the entire SPOCS compilation, and the value of  $\mathcal{P}_{\text{Ni}}$  is identical. This shows that our finding that planet hosts have enhanced silicon content was not the result of a selection effect. Here, the [Ti/Fe] distribution of the planet hosts is found to match that of the control set even more closely than when the experiment was performed on the entire SPOCS dataset, which underscores our finding that, for a given value of [Fe/H], titanium abundance is not correlated with the probability of finding a planet.

### 3. Empirical Model of Planet-[Si/Fe] Correlation

Having determined that planet hosts show evidence of silicon and nickel enhancement, we would now like to see if it is possible to empirically quantify the relationship between these abundances and probability of planet detection. Examination of Figure 3 reveals that once the planet hosts of SPOCS are binned according to iron abundance, small-sample statistics prevent us from robustly determining a planet-silicon or planet-nickel correlation. Any number of different functions could be used to fit the histograms in Figure 3, and the best fit would be noticeably different in each iron-abundance bin. While it is certainly possible, even likely, that the relationship between probability of planet detection and silicon/nickel abun-

dance changes with overall metallicity, it is not within our power to explore this empirically until more planet hosts have been discovered and surveyed.

We will use silicon as the test element to see whether or not we can empirically determine the relationship between probability of planet detection and  $[X/Fe]$  in the SPOCS data. We choose to test the simplest hypothesis: at a given metallicity, the probability of planet detection follows a power law in silicon abundance. We seek a model similar to the planet-metallicity correlation presented by Fischer & Valenti (2005), which uses the iron abundance:

$$P(\text{planet}) = 0.03 \times \left[ \frac{N_{\text{Fe}}/N_{\text{H}}}{(N_{\text{Fe}}/N_{\text{H}})_{\odot}} \right]^2 = 0.03 \times 10^{2.0[\text{Fe}/\text{H}]}.$$
 (2)

We therefore assume the following form for the planet-silicon correlation:

$$[P(\text{planet})]_{[\text{Fe}/\text{H}]} \propto 10^{b[\text{Si}/\text{Fe}]},$$
 (3)

where the notation  $[Y]_{[\text{Fe}/\text{H}]}$  denotes the quantity  $Y$  measured at constant  $[\text{Fe}/\text{H}]$ . The proportionality constant in equation 3 will be allowed to change with  $[\text{Fe}/\text{H}]$ , but the exponent  $b$  will not. We want to estimate the value of  $b$  implied by the SPOCS data set.

To do this, we again draw bootstrap realizations of the SPOCS data set, but we do not identify the actual planet hosts in each realization. Instead, we assign planets based on a two-dimensional probability distribution:

$$P(\text{planet}) = \mathcal{F}([\text{Fe}/\text{H}], [\text{Si}/\text{Fe}]).$$
 (4)

$\mathcal{F}$  is a two-dimensional histogram constructed such that each cut at constant  $[\text{Fe}/\text{H}]$  obeys equation 3. The proportionality constant for each  $[\text{Fe}/\text{H}]$  cut is set so that the planet-metallicity correlation remains intact:

$$\sum_{[\text{Si}/\text{Fe}]} \mathcal{F} = 0.03 \times 10^{2.0[\text{Fe}/\text{H}]}.$$
 (5)

We assume that each realization of the SPOCS data samples the entire range of  $[\text{Si}/\text{Fe}]$  values present in metal-rich stars, so equation 5 performs a discrete normalization of  $\mathcal{F}$ , such that  $\mathcal{F}$  is zero in regions of the  $[\text{Si}/\text{Fe}]$ - $[\text{Fe}/\text{H}]$  plane that contain no SPOCS stars. Using  $\mathcal{F}$ , we assign planets to the stars in each bootstrap realization of SPOCS, to simulate the relationship between planet detection and  $[\text{Si}/\text{Fe}]$  that would be present in SPOCS, if  $b$  were the proper exponent for equation 3.

As in §2, we create a control set with the same  $[\text{Fe}/\text{H}]$  distribution as the set of synthetic planet hosts, and use the K-S test to check for differences between the two sets'  $[\text{Si}/\text{Fe}]$



distributions. We perform 10, 10,000-simulation Monte-Carlo experiments, each with a different exponent  $b$  in equation 3 determining the form of  $\mathcal{F}$ . For each  $b$ , the Monte-Carlo simulations will tell us the distribution of probability that the set of synthetic planet hosts has the same silicon-abundance pattern as field stars with the same metallicity. We will call this distribution  $H$ . By comparing  $H$  with the previously determined distribution  $D_{\text{Si}}$ , we can find the exponent  $b$  that best models the planet-silicon correlation, as present in the SPOCS data. See Appendix B for a detailed description of the statistical methods used in these simulations.

Figure 4 shows the results of this experiment. Each panel shows  $H$  for a particular power-law exponent  $b$  that governs the planet-silicon correlation. Also plotted for comparison are  $D_{\text{Si}}$  and  $D_{\text{Fe}}$ , as shown in Figure 2. For  $b = 0$ , the null hypothesis in which likelihood of planet detection does not depend on silicon abundance except as it traces iron abundance (or overall metallicity),  $H$  closely follows the form of  $D_{\text{Fe}}$ , indicating that, as expected, the synthetic planet hosts and control stars with matching iron abundances follow the same  $[\text{Si}/\text{Fe}]$  distribution. As  $b$  increases,  $H$  gets more and more skewed toward low probabilities. The best match between  $H$  and  $D_{\text{Si}}$ , calculated by finding the value of  $b$  that corresponds to the maximum overlapping area under  $H$  and  $D_{\text{Si}}$ , is obtained with  $b = 7$ , so according to this analysis, the planet-silicon correlation has the form

$$[P(\text{planet})]_{[\text{Fe}/\text{H}]} \propto 10^{7[\text{Si}/\text{Fe}]}.$$
 (6)

Since  $[\text{Si}/\text{Fe}] = [\text{Si}/\text{H}] - [\text{Fe}/\text{H}]$ , equation 6 can be rewritten as

$$[P(\text{planet})]_{[\text{Fe}/\text{H}]} \propto 10^{7[\text{Si}/\text{H}]}.$$
 (7)

Such a strong correlation between silicon abundance and planet detection suggests an absolutely remarkable physical importance of silicon in the planet-formation process. It is unlikely, however, that silicon really is such a strong accelerant of planet formation, as a power-law exponent of seven indicates. Indeed, in Figure 4, varying  $b$  between 4 and 10 makes little difference in the form of  $H$ , which we take as evidence that either (1) a power law is not the correct form for the planet-silicon correlation, or (2) the SPOCS data do not robustly determine the relationships between probability of planet detection and  $[\text{X}/\text{Fe}]$ . No doubt such a strong difference in  $b$  would be obvious if stars at a given  $[\text{Fe}/\text{H}]$  could span a wide range in  $[\text{Si}/\text{Fe}]$ , but this is not the case, as we attach planets to observed values of  $[\text{Si}/\text{Fe}]$ . The sharper the planet-silicon correlation, the more the planet hosts merely get pushed to the top of the  $[\text{Si}/\text{Fe}]$  vs.  $[\text{Fe}/\text{H}]$  locus of Figure 1, until there are no higher values of  $[\text{Si}/\text{Fe}]$  available.

Rather than a power-law planet-silicon correlation with a large exponent, we suspect a threshold phenomenon: All circumstellar disks that can form Jovian planets do so, and the

division between disks that can form planets and those that cannot is a sharp cutoff, a step function in one parameter only. That one parameter may be silicon abundance itself, or it may be another physical quantity of which silicon is an indicator. If there were cutoff in silicon abundance, above which planets would definitely form and below which they could not, Figure 3 would show a step function in every panel. Instead, the step function is smeared out, so planets appear merely more frequently, rather than exclusively, around metal-rich and/or silicon-rich stars. Planet hosts and stars without planets occupy overlapping regions of the  $[\text{Fe}/\text{H}]-[\text{Si}/\text{Fe}]$  plane, suggesting that stars with high metallicity and high silicon abundance are more likely, but not guaranteed, to have protostellar disks that meet the criterion for planet formation. The exact value of the minimum silicon abundance required for planet formation must depend on the characteristics of the individual star-disk system. In the next section, we describe Monte Carlo simulations that predict frequency of planet formation based on iron abundance, silicon abundance, disk mass and radii, and disk lifetime. We will use a different method than the power-law fit presented in this section to compare our simulation results with the observed planet-silicon correlation.

#### 4. Probability of Planet Detection: Monte Carlo Simulations

In the core accretion model of planet formation, the critical quantity that controls whether gas giant planet formation can proceed is the solid surface density in the protostellar disk. A Jupiter-type planet will form if the disk has a sufficient concentration of solids just beyond the ice line for a protoplanetary core to reach runaway gas accretion before the disk dissipates (Pollack et al. 1996). If the disk solid surface density in the protoplanet’s feeding zone is too low for runaway gas accretion to begin, a Neptune-mass planet will form. According to the calculations by Hubickyj, Bodenheimer & Lissauer (in press), a Jupiter-mass planet can form in 2.3 Myr in a disk with solid surface density  $\sigma_{\text{solid}} = 10 \text{ g cm}^{-2}$  at 5 AU, whereas decreasing the surface density to  $\sigma_{\text{solid}} = 6 \text{ g cm}^{-2}$  increases the timescale for Jupiter formation to 13.3 Myr. Thus, a 40% decrease in solid surface density just beyond the ice line leads to a nearly 500% increase in Jupiter’s formation time, indicating a sharp threshold in the solid surface density required for giant planet formation in the Solar nebula. A disk enriched in either silicon or nickel would be more likely than its unenriched counterpart to be over the solid surface density threshold for planet formation.

The planet-metallicity correlation, modeled using the SPOCS data by Fischer & Valenti (2005), is a natural consequence of the core accretion theory of planet formation, since all solid species are metals. It has not yet been established whether  $[\text{Fe}/\text{H}]$  is a good predictor of planet detectability merely because it traces the total metal content of the star (i.e., all

metals are equally useful at forming planets), or because iron is a particularly important core-forming material. In the simplest interpretation of core accretion theory, the importance of each element to planet formation is in direct proportion to its abundance. The same multiplicative factor of enhancement over solar abundance adds the most solid mass when the enhanced element accounts for a large mass fraction of protoplanetary material. Correspondingly, depleting an otherwise metal-rich disk of a naturally abundant solid, such as oxygen, would seriously damage its chances for giant planet formation.

To illustrate the effect of different element enhancements on solid surface density, consider a disk with solar abundances of every element except iron. The disk has iron abundance double that of the sun ( $[\text{Fe}/\text{H}] = 0.3$ ), and its solid surface density is 12% higher than a disk with the same mass and inner and outer radii, but with Solar iron abundance (we use the solar abundances reported by Anders & Grevesse [1989], normalized to  $\log N_{\text{H}} = 12.00$ ). A disk with solar composition except for a factor of 2 enhancement of silicon, such that  $\log N_{\text{Si}} = 7.55 + 0.3$ , has solid surface density 6.7% higher than a disk with the same mass and radii, with solar composition. Doubling the abundance of nickel,  $\log N_{\text{Ni}} = 6.25 + 0.3$ , gives only a 0.7% increase in  $\sigma_{\text{solid}}$ . If the oxygen abundance of a disk with solar composition were doubled, keeping the same mass and radii, the solid surface density at the ice line would increase by 56%. Assuming carbon is present mainly in gaseous CO and CH<sub>4</sub> (Lewis & Prinn 1980), oxygen, iron and silicon are the elements that contribute the most solid mass to planet formation. The contribution of nickel, due to its low abundance, is much less significant. Galileo observations of Callisto and Ganymede, which formed outside the snow line of the proto-Jovian nebula, suggest that both are composed of  $\sim 50\%$  ice by mass (Sohl et al. 2002). Jupiter probably could not have formed in an oxygen-poor, yet iron-rich circumstellar disk.

We propose that there are two reasons why silicon abundance is correlated with planet detection: (1) silica and silicates form a significant portion of the grains that seed the planet formation process, silicon being the third most abundant solid element by mass at Jupiter’s position in the Solar nebula, and (2) most importantly, because silicon and oxygen are both  $\alpha$ -elements, the Si/O abundance ratio is roughly constant among metal-rich stars. Therefore,  $[\text{Si}/\text{Fe}]$  is a tracer of  $[\text{O}/\text{Fe}]$ , and silicon enrichment implies a star is oxygen-rich as well.

The link between silicon and oxygen abundance, and the preponderance of oxygen in protoplanetary material, prompted us to perform Monte Carlo simulations of the observed planet-silicon correlation. Our simulation combines observationally determined properties of protostellar disks, with new simulations, using the core accretion model, of planet-formation timescale as a function of solid surface density. We generate synthetic star-disk systems described by the independent random variables disk mass  $M_d$ , outer radius  $r_{\text{out}}$ , disk lifetime

$T$ ,  $[\text{Fe}/\text{H}]$  and  $[\text{Si}/\text{Fe}]$ . We do not simulate the effect of nickel enhancement on likelihood of planet formation. The solid surface density at Jupiter’s location in each disk is calculated from the disk mass and chemical composition. If the solid surface density is high enough for a protoplanetary core to reach runaway gas accretion within the disk lifetime, the star becomes a planet host. We generate 100,000 star-disk systems, which we use to quantify the relationship between probability of planet detection and silicon abundance. Our results should reproduce both the planet-metallicity correlation and the trend reported in this paper, of planets being found preferentially around silicon-rich stars.

In §4.1, we give the results of new numerical simulations that model the relationship between disk solid surface density and timescale for planet formation. In §4.2, we describe the random variables that specify star-disk systems in our Monte Carlo simulations. Finally, in §4.3, we discuss our simulations’ predictions about  $\alpha$ -enrichment in planet hosts, and compare these predictions with the trends present in the SPOCS data.

#### 4.1. Solid Surface Density and Timescale for Planet Formation

We use the theoretical model of planet formation described by Laughlin, Bodenheimer & Adams (2004, hereafter LBA) to calculate planet formation timescale as a function of solid surface density. Initially, a protoplanetary core of mass  $M_{\oplus}$  is embedded at 5.2 AU in a disk of age  $10^5$  years, surrounding a T-Tauri star of mass  $1M_{\odot}$ . This is a good match for the SPOCS data, which, consisting of FGK stars, have a median stellar mass of  $1.14M_{\odot}$ . The disk is flat and passive, and isothermal in the vertical direction. The stellar effective temperature  $T_*(t, M_*)$  and luminosity  $L_*(t, M_*)$  are adopted from published pre-main-sequence stellar evolution tracks (D’Antona & Mazzitelli 1994).

The contraction and buildup of protoplanetary cores and their gaseous envelopes embedded in our model evolving disk are computed with a Henyey-type code (Henyey et al. 1964). Following the argument of Podolak (2003) that grain settling in the protoplanetary envelope would reduce envelope opacity where grains exits, we adopt grain opacities of  $\sim 2\%$  of the interstellar values used in Pollack et al. (1996). We use a core accretion rate of the form  $dM_{\text{core}}/dt = C_1 \pi \sigma_{\text{solid}} R_c R_h \Omega$  (Papaloizou & Terquem 1999), where  $\sigma_{\text{solid}}$  is the surface density of solid material in the disk,  $\Omega$  is the orbital frequency at 5.2 AU,  $R_c$  is the effective capture radius of the protoplanet for solid particles,  $R_h = a[M_{\text{planet}}/(3M_*)]^{1/3}$  is the tidal radius of the protoplanet (where  $a$  is the semimajor axis of the protoplanet’s orbit), and  $C_1$  is a constant near unity. The outer boundary conditions for the protoplanet include the decrease with time in the background nebular density and temperature.

One parameter in the model is the gas/solid ratio just beyond the ice line in the Solar nebula, at the onset of protoplanetary core formation. To find the gas/solid ratio, we assume the Solar elemental abundances of Anders & Grevesse (1989) and follow the chemical model of Hersant, Gautier & Lunine (2004, hereafter HGL). As in Lewis & Prinn (1980), we assume all carbon in the pre-solar nebula was in CO and CH<sub>4</sub>, all oxygen was in CO and H<sub>2</sub>O, and all nitrogen in N<sub>2</sub> and NH<sub>3</sub>. If the CO/CH<sub>4</sub> ratio in the pre-solar cloud was preserved in the Solar nebula, CO/CH<sub>4</sub> = 10. HGL present stability curves for the CHON ices, which show that CO at 5 AU does not freeze until  $\sim 3$  Myr after disk formation, nor become trapped in clathrate hydrates until 1.6 Myr after disk formation, by which the protoplanet has already started to build up a gaseous envelope (LBA). CH<sub>4</sub> freezes at 2.8 Myr and clathrates at 1.3 Myr, by which time  $\sim 1/2$  of the core mass has already accumulated. The only volatile besides H<sub>2</sub>O that could possibly freeze or clathrate while the solid core is truly embryonic is NH<sub>3</sub> at 0.9 Myr. However, at N<sub>2</sub>/NH<sub>3</sub> = 10 (Lewis & Prinn 1980, Irvine & Knacke 1989), NH<sub>3</sub> comprises such a minor proportion of the CNO-bearing molecules that it cannot significantly speed up the formation of protoplanetary cores.

We therefore assume that all CNO species except water are in the gas phase. Although carbon can form refractory organic compounds, these should be present in small amounts compared to CO (see, however, Lodders 2004). Considering elements with abundances  $10^6$  and above (relative to  $N_H = 10^{12}$ ), we assume solid Na, Mg, Al, Si, Ca, Fe and Ni. We also assume solid sulfur, in the form of FeS and H<sub>2</sub>S. According to Pasek et al. (2005), the condensation front of troilite (FeS) is between 1 and 2 AU from the Sun at the start of our simulations,  $10^5$  years after Solar-nebula formation. H<sub>2</sub>S is half frozen at the snow line, and continues to solidify as the disk evolves. Two hydrogen atoms for every oxygen bound in H<sub>2</sub>O are frozen as well, and He, C, N, Ne and Ar are entirely in the gas phase. At Solar abundances and with CO/CH<sub>4</sub> = 10, 62% of the oxygen atoms are frozen in H<sub>2</sub>O, and the rest are in CO gas. This gives an initial gas/solid ratio just beyond the ice line in the Solar nebula of  $G/S = 100$ , adjusted from  $G/S = 70$  in LBA. The model accounts for the decrease in  $G/S$  with time as gas evaporates from the disk using the same functional form as LBA.

We calculated the time to runaway gas accretion for different initial values of solid surface density. At  $\sigma_{\text{solid}} = 5.5, 7.5, 9.5, 11.5$  and  $13.5 \text{ g cm}^{-2}$ , the times to accelerating accretion are 9.2, 5.3, 4.1, 3.2 and 2.5 Myr, respectively. To describe planet formation time as a function of surface density, we fit an power law to the simulation results:

$$t_{\text{rga}} = \left( \frac{\sigma_{\text{solid}}}{25.0 \text{ g cm}^{-2}} \right)^{-1.44} \quad (8)$$

where  $t_{\text{rga}}$  is the time to rapid gas accretion in Myr. The simulation results and the fit in equation 8 are plotted in Figure 5. For the synthetic star-disk systems in our Monte Carlo

simulation, if  $t_{\text{rga}}$  is less than the disk lifetime, a giant planet forms.

## 4.2. Disk Properties

Since surface density and disk lifetime together determine whether Jovian planets can form, we seek to describe these in terms of independent, random variables that can be the basis of Monte Carlo simulations. If one assumes (1) that disk lifetime does not depend on disk mass, both of these can be chosen as random variables in the simulations. We have no observational information about what the surface density 5 AU from protostars might be, so we make the further assumption (2) that, although the outer disk radius may vary, the disks always have the same inner radius and surface density distribution (gas+solid) is always characterized by the same power law in radius. If we assume (3) abundances in stars are the same as in their circumstellar disks, and (4) that the  $[X/\text{Fe}]$  ratios of all  $\alpha$ -elements are roughly the same in all metal-rich stars, such that  $[\text{Si}/\text{Fe}] = [\alpha/\text{Fe}]$ , we can specify a star-disk system with two more random variables that have observational constraints:  $[\text{Fe}/\text{H}]$  and  $[\text{Si}/\text{Fe}]$ .

Observations of IC 348 by Haisch, Lada & Lada (2001a) indicate that disk lifetime in the cluster may depend on the spectral type of the star: No circumstellar disks were detected around OBAF T-Tauri stars, suggesting that these disks have shorter lifetimes than the disks surrounding late-type stars. Statistically, this would lead to shorter lifetimes for higher-mass disks, since disk mass is directly correlated with star mass (Briceño et al. 2001). However, no difference in disk frequency between G and K T-Tauri stars was detected by Haisch, Lada & Lada (2001a), nor was the ratio of (accreting) CTTSs, to (presumed diskless) WTTSs in Taurus-Auriga found to vary with age (Kenyon & Hartmann 1995). We wish to simulate the frequency of planet formation by late F, G and K dwarfs, since more massive stars are excluded from radial-velocity planet searches, including SPOCS. Therefore, we conclude that, within the domain of our simulation, assumption (1) is justified.

Assumption (3) is implicit because we are using the silicon abundance observed by SPOCS in evolved, main-sequence stars to determine whether conditions in a star’s accretion disk were right for planet formation. Our simulation assumes that disks do not fractionate in element abundances, at least within 5.2 AU of their protostar. We must also assume that the silicon initially present in a star’s photosphere does not significantly settle inward during the star’s main-sequence lifetime. However, the agreement between photospheric and meteoritic silicon abundance in the Solar system (Anders & Grevesse 1989) indicates that stellar silicon abundance can be used to diagnose conditions in planet-forming disks.

Assumption (4) is the basis for the assertion that disk mass, [Si/Fe], and [Fe/H] fully specify the amount of solid material available for planet formation. We assume that the  $\alpha$ -elements are present in the same proportions in all metal-rich stars. The most important  $\alpha$ -element in our simulation is oxygen, since it is the most abundant solid material in planet-forming disks. Soubiran & Girard (2005) find that the  $\alpha$ -elements Mg, Si, Ti and Ca in thin- and thick-disk stars show similar behavior in the [X/Fe] vs. [Fe/H] plane, with [X/Fe] flattening and staying relatively constant above solar metallicity. However, they find that oxygen shows a decreasing trend at high metallicity. Feltzing & Gustafsson (1998) also find that [O/Fe] continues to decline at [Fe/H]  $\geq$  0.0, which does not match the trend in [Si/Fe] either in their own data or in the SPOCS data (see Figure 1). However, the models of Prantzos & Aubert (1995) predict [O/Fe] flattening at solar metallicity, which is supported by the observations of Nissen & Edvardsson (1992). It appears that the evolution of [O/Fe] at high metallicity is not fully understood, but as long as we may at least say that silicon traces oxygen and the other  $\alpha$ -elements *better* than iron does, we have a basis for assumption (4).

We argue, therefore, that a planet-forming star-disk system can be described by five random variables: disk mass, outer radius, disk lifetime, [Fe/H] and [Si/Fe]. §4.2.1, 4.2.2 and 4.2.3 describe the observationally motivated distributions from which these random variables are chosen.

#### 4.2.1. Disk Mass, Radius and Surface Density Profile

To characterize the distribution of disk masses around pre-Solar stars, we first assume that a large number of independent processes determine the disk mass as the star evolves toward the T-Tauri phase. For example, the behavior of protostellar collimated outflows, which largely control the envelope dissipation rate during the Class I phase, depends on the strength of the magnetic field threading the disk (see, e.g., Shu et al. 1995) and the accretion rate onto the star (Calvet 2003). If sufficiently many of the processes that control disk mass at the start of planet formation are described by independent random variables, the disk mass distribution naturally assumes a lognormal form. This characterization follows the same reasoning as Adams & Fatuzzo (1996), who invoked the central limit theorem to model the stellar IMF as a lognormal distribution.

The fiducial point of the disk mass distribution is determined from the observations of Andrews & Williams (2005). Their survey of 153 young stellar objects in the Taurus-Auriga star-forming region revealed a lognormal distribution of disk masses with a mean mass of  $\sim 5 \times 10^{-3} M_{\odot}$  and a median disk-to-star mass ratio  $M_d/M_* = 0.5\%$ . This result is consistent

with Osterloh & Beckwith (1995), who found a median ratio  $M_d/M_* = 0.45\%$  for the 16 classical T-Tauri stars in their sample. In our core accretion simulations, the gas surface density decreases as  $\sigma_{gas} \propto 1/t$ . Our simulations begin at  $t = 10^5$  years, so after  $10^6$  years, the gas disk mass has decreased by a factor of 10. Since the disks in Taurus-Auriga are between 1 and 2 Myr old (Kenyon & Hartmann 1995), we assume that the disks studied by Andrews & Williams (2005) began their lives with 10 times more mass than they are currently observed to possess. Therefore, the fiducial point of our disk mass distribution is  $M_d = 0.05M_\odot$ .

Andrews & Williams (2005) found that the dispersion in disk mass is 0.5 dex. However, some of this scatter must be accounted for by the large range of protostar ages in their sample: According to Kenyon & Hartmann (1995), stars have been forming at a constant rate in Taurus-Auriga for the last 1-2 Myr. Work by Shu et al. (1990) and Laughlin & Rozyczka (1996) suggests that disks with  $M_d > 0.3M_*$  are gravitationally unstable to non-axisymmetric disturbances, and will rapidly evolve via accretion to lower-mass configurations. Even a disk of mass  $0.1M_*$  can experience low-level gravitational instability, leading to clumping and fragmentation, if the cooling time is on the order of local dynamical time anywhere in the disk (Rice, Lodato & Armitage 2005, Boss 2002). In a lognormal distribution with median  $0.05M_\odot$  and standard deviation 0.5 dex, 27% of disks have initial mass  $M_d > 0.1M_*$ . These disks may be likely to fragment and form binary star systems. After fragmentation, planet formation by core accretion could proceed, but the resulting circumbinary disk would be substantially reduced in mass, as the original disk would have donated much of its mass to the newly formed red or brown dwarf.

In addition, a large dispersion in disk mass raises the likelihood that even a low-metallicity disk will form a Jovian planet, because the disk has a high chance of being massive enough to compensate for a low metal abundance. Running the simulation with a disk mass dispersion of 0.5 dex produces a set of synthetic star-disk systems with no apparent relation between  $[\text{Fe}/\text{H}]$  and likelihood of planet formation. Since the planet-metallicity correlation has been well established by observations, we argue that the spread in initial disk masses around FGK dwarfs, at the beginning of the T-Tauri phase, is probably not as large as 0.5 dex. We select a standard deviation of 0.25 dex for our disk mass distribution, which means that the violent, global gravitational instability of  $0.3M_*$  disks is a  $3\sigma$  event.

The core accretion simulations presented in §4.1 do not involve planetary migration, and hence do not assume any particular surface density profile in the protostellar disk: The planet could be forming in a region of the disk with locally enhanced or depleted surface density. To convert from disk mass to surface density (solid+gas), we adopt a truncated disk



with a surface density profile

$$\sigma(r) = \sigma_{in}(r_{in}/r)^{3/2}, \quad (9)$$

(Weidenschilling 1977). For the surface density profile to integrate to a disk of mass  $M_d$ , the surface density at the inner boundary must be

$$\sigma_{in} = \frac{M_d/4\pi r_{in}^2}{(r_d/r_{in}) - 1}. \quad (10)$$

To find reasonable values for the inner and outer disk radii, we look first to the mass distribution in the Solar system. Since the mass of the terrestrial planets is less than 1% of the mass of the giant planets, one possible disk configuration can be calculated by assuming the entire disk mass is contained in a region just encompassing the orbits of Jupiter and Neptune, with  $r_{in} = 4.5$  AU and  $r_{out} = 36$  AU. We adopt  $r_{in} = 4.5$  AU for all synthetic star-disk systems. Determination of disk outer radii by near-infrared observations, even from space, is limited by angular resolution, which is not sufficient to probe inside 100 AU for all but the nearest T-Tauri stars. The study of the Trapezium cluster by Vicente & Alves (2005) indicates that  $\sim 40\%$  of disks have radius larger than 50 AU, with a power-law falloff in disk diameter beyond 50 AU. However, observations of TW Hydrae (Weinberger et al. 2002) and GM Aurigae (Schneider et al. 2003) indicate outer disk radii of  $\sim 150$  AU. We adopt the flat distribution  $36 < r_{out} < 100$  AU for outer disk radii in our simulation.

Once the disk mass and outer radius are specified, we use equation 9 to calculate the surface density (gas and solid) at 5.2 AU from the protostar.

#### 4.2.2. Disk Lifetime

There are many distinct processes that contribute to the disk dissipation rate in the classical T-Tauri phase. The gas photoevaporation rate depends not only on the protostar's accretion luminosity, but on the radiation environment of the entire star-forming region. Even if dust coagulates quickly enough to form planetesimals, disk gas in dense clusters may be dispersed before runaway accretion can begin (Hollenbach & Adams 2004). Nearby, massive stars likely accelerate disk dissipation as well (Johnstone et al. 1998). Photoevaporating winds may also carry micron-size dust grains away from the disk before they can build larger grains, cutting off protoplanetary core mass below the threshold of runaway accretion.

We therefore assume that protostellar disk lifetime  $T$  follows a lognormal distribution. This is consistent with the observations of Haisch, Lada & Lada (2001b), who used *JHKL* color-color diagrams to derive the disk frequency in open clusters of different ages, finding

that disk frequency decreases rapidly with cluster age. By combining their data with previous observations of open clusters (Haisch, Lada & Lada 2000, Kenyon & Hartmann 1995, and Kenyon & Gómez 2001), Haisch, Lada & Lada (2001b) found that half of disks are lost by an age of 3 Myr, and almost all disks dissipate by 6 Myr. We therefore set the fiducial disk lifetime at 3 Myr. In specifying the standard deviation of the disk mass distribution, we must account for the longevity of disks such as those in the TW Hydra association, of age 5-15 Myr (Weintraub et al. 2000), or  $\eta$  Cha cluster, with accreting disks up to 10 Myr old (Lawson, Lyo & Feigelson 2003). These disks are observationally rare, but this may be a selection effect, because the detection of pre-main-sequence objects is biased toward young, massive disks (Lawson, Lyo & Feigelson 2003). We therefore set the spread of the disk lifetime distribution at 0.15 dex, which places 6 Myr disks at  $2\sigma$  above the fiducial, and the 10 Myr disks of  $\eta$  Cha at  $3.5\sigma$  above the fiducial disk lifetime.

#### 4.2.3. Chemical Composition and Calculation of Solid Surface Density

The chemical composition of our star-disk systems was specified by [Fe/H] and [Si/Fe], which we assume to be equal to  $[\alpha/\text{Fe}]$ . These, in conjunction with the chemical model of HGL and equation 9, specify the solid surface density at Jupiter’s distance from the Sun. We consider only elements with sufficient abundance in the sun (according to Anders & Grevesse 1989) that  $N_X \geq 10^{-6}N_H$ , where  $N_X$  is the number of atoms of a element X present in one cubic centimeter of disk material, and  $\log N_{H,\odot} = 12.00$ . The elements in our simplified star-disk systems are therefore H, He, C, N, O, Ne, Na, Mg, Al, Si, S, Ar, Ca, Fe and Ni, of which He, C, O, Ne, Mg, Si, S, Ar and Ca are  $\alpha$ -elements or related products of helium burning.

$\alpha$ -abundances for our star-disk systems cannot be selected independently of [Fe/H], since Galactic chemical evolution assures that  $[\alpha/\text{Fe}]$  will depend on [Fe/H] (Timmes, Woosley & Weaver 1995). To use  $[\alpha/\text{Fe}]$  as a random variable in our simulation, we use the Fischer & Valenti (2005) subset of SPOCS with a uniform probability of planet detection to empirically model [Si/Fe] vs. [Fe/H]. We first fit a fourth-order polynomial to [Si/Fe] as a function of [Fe/H] in the uniform set:

$$[\text{Si}/\text{Fe}] = -0.00516 - 0.162[\text{Fe}/\text{H}] + 0.449[\text{Fe}/\text{H}]^2 - 0.377[\text{Fe}/\text{H}]^3 - 0.974[\text{Fe}/\text{H}]^4. \quad (11)$$

We subtract this fit to find the iron abundance-independent [Si/Fe] residuals  $\Delta[\text{Si}/\text{Fe}]$ . The polynomial fit and residuals are plotted in Figure 6. We then fit a Cauchy distribution to a histogram of  $\Delta[\text{Si}/\text{Fe}]$ :

$$P(\Delta[\text{Si}/\text{Fe}]) = C \left( \frac{(1/2)\Gamma}{(\Delta[\text{Si}/\text{Fe}] - (\Delta[\text{Si}/\text{Fe}])_0)^2 + ((1/2)\Gamma)^2} \right), \quad (12)$$

where  $C = 0.0254$ ,  $(\Delta[\text{Si}/\text{Fe}]_0) = 0.00600$  is the center of the distribution, and  $\Gamma = 0.0445$ . This fit is shown in Figure 7. The fact that the center of the residual distribution is so close to zero means the fiducial sequence  $[\text{Si}/\text{Fe}]$  as a function of  $[\text{Fe}/\text{H}]$  is well modeled. Since we assume  $[\alpha/\text{Fe}] = [\text{Si}/\text{Fe}]$ , the Cauchy distribution describing  $\Delta[\text{Si}/\text{Fe}]$  is the distribution from which the random variable describing  $\alpha$ -abundance is drawn.

The synthetic star-disk systems are initially given Solar abundances. Then iron abundance of each synthetic star-disk system is selected from a uniform distribution within the limits  $-0.7 \leq [\text{Fe}/\text{H}] \leq 0.5$ . All known extrasolar planets orbit stars within this range. The abundances of all metals are then altered by a factor of  $[\text{Fe}/\text{H}]$ :

$$N_{\text{M}} = 10^{[\text{Fe}/\text{H}]} N_{\text{M},\odot}, \quad (13)$$

where  $N_{\text{M}}$  denotes metal abundance. Using equation 11, the fiducial value of  $[\alpha/\text{Fe}]$  for the selected  $[\text{Fe}/\text{H}]$  is calculated. From the distribution in equation 12, we then select the  $\alpha$ -adjustment factor  $\Delta[\alpha/\text{Fe}]$ . We are then ready to specify  $[\alpha/\text{Fe}]$  for the star-disk system:

$$[\alpha/\text{Fe}] = [\alpha/\text{Fe}]_{\text{fiducial}} + \Delta[\alpha/\text{Fe}]. \quad (14)$$

The individual  $\alpha$ -element abundances for the star-disk system are then altered by a factor of  $[\alpha/\text{Fe}]$ :

$$N_{\alpha} = 10^{[\alpha/\text{Fe}]} N_{\alpha,0}. \quad (15)$$

Once the abundances of all the elements in the star-disk system are specified, we can calculate the gas/solid ratio at the snow line. As in §4.1, the solid elements are Na, Mg, Al, Si, S, Ca, Fe, Ni, 62% of oxygen and the hydrogen bound up in  $\text{H}_2\text{O}$ . The gas/solid ratio is calculated as

$$G/S = \frac{\sum_X (1 - S_X) W_X N_X}{\sum_X S_X W_X N_X}, \quad (16)$$

where  $W_X$  is the atomic weight of element X,  $S_X$  is the fraction of X that is solid at the ice line, and  $N_X$  is the abundance of X. Knowing the gas/solid ratio and the total surface density at 5.2 AU calculated from equation 9, we can then calculate the solid surface density:

$$\sigma_{\text{solid}} = \frac{\sigma}{(G/S + 1)}. \quad (17)$$

As one example of the relationship between  $[\text{Si}/\text{Fe}]$  and  $\sigma_{\text{solid}}$  in our simulation, a disk with  $[\text{Fe}/\text{H}] = 0.0$  and  $[\text{Si}/\text{Fe}] = 0.3$  has solid surface density 37% higher than a disk with the same mass and outer radius, with  $[\text{Fe}/\text{H}] = 0.0$  and  $[\text{Si}/\text{Fe}] = 0.0$ . This is less than the solid surface density obtained by increasing only oxygen abundance because helium and carbon, gaseous  $\alpha$ -elements, have their abundances increased along with silicon and oxygen.

At this point, we have specified the solid surface density and the lifetime of our synthetic star-disk system. Using equation 8, we calculate the timescale for planet formation. If this timescale is less than the protostellar disk lifetime, a planet forms. By building  $10^7$  synthetic star-disk systems and analyzing their properties, we now perform a theoretical test of the planet-silicon correlation and compare the results with the trends observed in the SPOCS data.

### 4.3. Simulation Results

In this section, we present the results of our Monte Carlo simulations. We assess how well the simulations reproduce the observed planet-metallicity correlation. We then use the disk lifetime and time to rapid gas accretion from our simulations to predict the fraction of Jovian planets that do not migrate, and therefore may dominate planetary systems similar to our own. Next, we estimate the fraction of Saturn analogs at 5 AU from their parent star, and use our relation between solid surface density and time to rapid gas accretion to calculate the lifetime of the solar nebula. Finally, we examine the planet-silicon correlation as predicted by our simulations and speculate on other elements that might correlate with likelihood of planet formation.

#### 4.3.1. Planet-Metallicity Correlation

The first test of our simulation is whether it reproduces the planet-metallicity correlation. This correlation has been well established by many observers (e.g Fischer & Valenti 2005), and has also been reproduced by other semi-analytic planet formation models in the literature, including those of Ida and Lin (2004a, 2004b, 2005) and Kornet et al. (2005). Both the Ida & Lin and the Kornet et al. theories incorporate results from core accretion calculations that are very similar to those used in our simulation. In particular, all three theories contain a phase of rapid gas accretion, whose time of onset depends sensitively on the solid surface density. Hence, for a given disk mass and lifetime, these theories naturally produce a connection between host-star metallicity and the presence of a detectable Jovian-mass planet. The Ida-Lin theory also explicitly reproduces the observed paucity of planets with masses that fall in the  $100 - 200M_{\oplus}$  range, in which rapid gas accretion is expected to occur most easily.

We calculate the fraction of stars in each metallicity bin that have planets, and compare with equation 2, derived by Fischer & Valenti (2005). Figure 8 shows that our simulation

reproduces the increasing trend in number of planets with  $[\text{Fe}/\text{H}]$ . However, above super-Solar metallicity, our simulation shows the slope of the planet-metallicity correlation changing from increasing with  $[\text{Fe}/\text{H}]$  to decreasing with  $[\text{Fe}/\text{H}]$ . The planet-metallicity correlation takes the form of a logistic curve, as expected for a monotonically increasing relation bounded by 0% (no stars form planets) and 100% (all stars form planets). Indeed, it appears that above  $[\text{Fe}/\text{H}] = 0.3$ , the slope of our theoretical planet-metallicity correlation starts to flatten. We determine the following equation for the probability that the disk surrounding a star of metallicity  $[\text{Fe}/\text{H}]$  ever had a giant planet companion:

$$P(\text{planet}) = \frac{1}{7.86(0.00493^{[\text{Fe}/\text{H}]} + 1.00)} \quad (18)$$

The inflection point of equation 18 is at  $[\text{Fe}/\text{H}] = 0.38$  dex. At  $[\text{Fe}/\text{H}] = 0.38$  dex, fiducial  $[\alpha/\text{Fe}] = -0.04$ , and given an accretion disk with our simulation’s fiducial disk mass ( $M_d = 0.05M_\odot$ ), and the median outer radius in our simulation (68 AU), the solid surface density at Jupiter’s distance from the sun is  $\sigma_{\text{solid}} = 11.1 \text{ g cm}^{-2}$ . This is on the section of the planet formation timescale curve in Figure 5 where  $t_{\text{rga}} < 3$  Myr, where a large increase in  $\sigma_{\text{solid}}$  lowers the formation time only slightly. Above  $[\text{Fe}/\text{H}] = 0.38$  dex, therefore, increasing metallicity, despite the fact that it increases solid surface density, can longer profoundly increase the probability of planet formation.

#### 4.3.2. Long-Period vs. Short-Period Planets

Our simulations predict that 16% of FGK dwarfs have giant planets, in rough agreement with Marcy et al. (2005), who conclude that  $\sim 12\%$  of FGK dwarfs should have planets. Marcy et al. (2005) used a flat extrapolation between 5 and 20 AU of the observed distribution of planet frequency vs. semimajor axis to predict the frequency of giant planets around FGK dwarfs. This distribution of planet frequency as a function of semimajor axis in the Lick/Keck/AAT planet search data is not well constrained. Only 47 of the planet hosts in these data had at least 10 observations, with precision  $30 \text{ m s}^{-1}$ , spanning four years. The decline in planet frequency above semimajor axes of 3 AU may thus be an artifact of the finite time baseline of the observations. Marcy et al. (2005) report increasing incompleteness of the data beyond 3 AU.

We can calculate the difference between protostellar disk lifetime and time to rapid gas accretion,  $L - t_{\text{rga}}$ , and compare this quantity with Type II migration timescales in the literature. This way, we can use our simulation results to estimate of the fraction of Jupiter-mass planets that stay approximately at their formation radius, and do not migrate.

Estimating the number of Jovian-mass planets that do not migrate gives an upper limit to the number of planetary systems that might be Solar System analogs. It also has implications for the yield of long time-baseline Doppler surveys. For Jovian planets to be detected by radial-velocity searches, the gas in the disk had to remain long enough after the planet reached approximately Jovian mass to force the planet to migrate inward. Nelson et al. (2000), D’Angelo, Kley & Henning (2003) and Papaloizou & Nelson (2005) are all in agreement that the migration timescale of a Jupiter-mass planet at 5.2 AU from the sun is  $10^4$  orbital periods, or  $\sim 10^5$  years. The long-period planets in our simulation, which never experience Type II migration, are those in which the planet reached rapid gas accretion less than  $10^5$  years before the disk dissipated. These account for 4% of the planets formed in our Monte Carlo simulations. True Solar-System analogs, therefore, likely make up only a small percentage of the planetary systems that initially formed in the Solar neighborhood, though they may account for a higher percentage of planetary systems that survived to maturity, since some giant planets end Type II migration by colliding with their parent stars (Ida & Lin 2004b).

Even as we predict a higher frequency of planets than has been observed, as expected from lack of completeness for long periods in Doppler surveys, when we compare our theoretical planet-metallicity correlation with the observations of Fischer & Valenti (2005), we find that the discrepancy between our simulation and observations is highest at low metallicities (Figure 8). At  $[\text{Fe}/\text{H}] = -0.2$ , we predict the frequency of giant planet formation is 3.5 times what is observed, whereas at  $[\text{Fe}/\text{H}] = 0.4$ , we predict this frequency is only 2.7 times what is observed. Low-metallicity disks that manage to form planets are more likely than their high-metallicity counterparts to dissipate soon after the planets have reached rapid gas accretion, due to the overall longer timescale of planet formation in these disks. This would explain our simulations’ prediction of a higher number of planets than observed being more pronounced at low metallicities. We assume planets that finish forming less than the Type II migration timescale before disk dissipation, and thus do not migrate, are long-period planets, while the rest are short-period planets. Metal-poor disks, therefore, have a higher probability of forming as yet undetected long-period planets than metal-rich disks. Figure 9 compares the  $[\text{Fe}/\text{H}]$  distribution of the host stars of long-period and short-period planets in our simulation results. The  $[\text{Fe}/\text{H}]$  distribution of short-period planets is more strongly skewed toward high metallicities than that of long-period planets.

#### 4.3.3. *Saturn-Mass Planets at 5 AU*

The combination of the core accretion process of planet formation and rapid dissipation of gas in protostellar disks would allow for the existence of planets like Saturn, which has

a mass consistent with having suddenly stopped gathering an envelope in the middle of its rapid gas accretion phase. One formation scenario for Jupiter that is consistent with core accretion theory is that Jupiter was embedded in a disk in which a substantial amount of gas remained for 5.2 Myr, then suddenly dissipated before the planet could experience Type II migration; Jovian planets are then the result of a coincidence between the gas dissipation epoch and the rapid gas accretion stage of planet formation. (If Jupiter and Saturn were nearer each other than their 2:1 mean motion resonance, this would also prevent substantial inward migration; see Morbidelli, Crida & Masset [2005].) The Jupiter-migration timescale of  $10^5$  years would then also be the upper limit on gas dissipation time in a rapid-dissipation scenario. Papaloizou & Nelson (2005) calculate that once a planet has reached the rapid gas accretion phase (having a typical mass of  $\sim 30M_{\oplus}$ , in agreement with LBA), a Jupiter mass of gas can be accreted in  $10^3$  years, for 1% interstellar dust opacity. Saturn-mass planets, if they indeed are the result of gas dissipation occurring during the *middle* of rapid gas accretion, should then account for  $10^3/10^5 = 1\%$  of the population of giant planets on ten-year orbits. This speculation, of course, does not take into account the effects of two embryos competing for gas, which could also suddenly cut off rapid gas accretion.

#### 4.3.4. Nature of the Solar Nebula

We now use our numerical simulations of the relationship between  $\sigma_{\text{solid}}$  and  $t_{\text{rga}}$  to speculate on the nature of the Solar nebula. Saumon and Guillot (2004) conclude that the upper limit on solid surface density during Jupiter’s formation should be  $8 \text{ g cm}^{-2}$ , based on the abundances of heavy elements in Jupiter’s envelope. Based on our core accretion simulations, this corresponds to a time to rapid gas accretion of 5.2 Myr. Our simulations therefore predicts that the lifetime of the Solar nebula was  $1.6\sigma$  above that of the average Population I disk. The Sun’s formation environment, therefore, may have been somewhat more quiescent than typical. Assuming the distribution of mass in the Solar nebula roughly matches that of the Solar system today, the inner and outer disk radii during Jupiter’s formation were at 4.5 and 36 AU, just encompassing the orbits of Jupiter and Neptune. This gives the total mass of the Solar nebula as  $0.05M_{\odot}$ . Figure 10 gives the percent of stars that form Jovian-mass planets as a function of disk mass  $M_d$  and lifetime  $T$ . According to our Monte Carlo simulations, 27% of disks with the lifetime of the Solar nebula will form planets, whereas only 10% of disks with the mass of the Solar nebula will form planets. Since the Sun is neither particularly metal-rich, in comparison to the population of planet hosts, nor  $\alpha$ -rich, the critical factor that allowed planets to form in the Solar nebula was its long lifetime.

#### 4.3.5. Planet-Silicon Correlation

Most importantly, our simulations predict that stars with planets are silicon-enhanced. Figure 11 shows histograms of the fraction of stars with planets as a function of  $[\text{Si}/\text{H}]$ , in different  $[\text{Fe}/\text{H}]$  bins. Instead of a power law with a large exponent, the probability of planet formation appears to increase linearly with  $[\text{Si}/\text{Fe}]$  at a constant value of  $[\text{Fe}/\text{H}]$ , or logarithmically with silicon abundance. There is some sign that the planet-silicon correlation assumes a logistic form (as, with finite top and bottom bounds, it should), especially in the  $[\text{Fe}/\text{H}]$  range  $-0.15 < [\text{Fe}/\text{H}] < 0.05$ . The planet-silicon correlation is steeper at higher  $[\text{Fe}/\text{H}]$ . We model the correlation as the linear function

$$[P(\text{planet})]_{[\text{Fe}/\text{H}]} = C + A[\text{Si}/\text{Fe}], \quad (19)$$

$P$  is the percent of stars with planets where  $C$  is a constant reflecting the change in the total number of planets expected to form in each  $[\text{Fe}/\text{H}]$  bin. For  $[\text{Fe}/\text{H}] = -0.15, -0.05, 0.05, 0.15, 0.25$  and  $0.35$ , the slope  $A$  of the planet-silicon correlation is 0.19, 0.32, 0.47, 0.60, 0.66 and 0.67. The increasing slopes may reflect that the low- $[\text{Fe}/\text{H}]$  bins include some of the flat bottom of the logistic curve.

At this point, we would like to assess how well the planet-silicon correlation predicted by our simulations matches the SPOCS data. As discussed in §3, the small number of planet hosts in SPOCS prevent us from merely binning the data by  $[\text{Fe}/\text{H}]$  and measuring the planet-silicon correlation in each bin, as we did in Figure 11 for our simulation results. However, the fiducial value of  $[\text{Si}/\text{Fe}]$  predicted by equation (11) changes little in the range  $0.05 < [\text{Fe}/\text{H}] < 0.35$ : here,  $[\text{Si}/\text{Fe}]$  vs.  $[\text{Fe}/\text{H}]$  is almost flat. We can, therefore, measure the planet-silicon correlation in the SPOCS data using the 447 stars, including 56 planet hosts, in this  $[\text{Fe}/\text{H}]$  range.

Figure 12 compares the planet-silicon correlation predicted by our simulations with that present in the SPOCS data for stars with  $0.05 < [\text{Fe}/\text{H}] < 0.35$ . Modeling the SPOCS planet-silicon correlation with a linear fit *over the range of  $[\text{Si}/\text{Fe}]$  values where planets have been found* ( $-0.1 < [\text{Si}/\text{Fe}] < 0.1$ ) gives the equation

$$P(\text{planet})_{\text{SPOCS}} = 0.13 + 0.55[\text{Si}/\text{Fe}]. \quad (20)$$

A linear fit to the theoretical planet-silicon correlation implied by our simulations for all values of  $[\text{Si}/\text{Fe}]$  in the range  $0.05 < [\text{Fe}/\text{H}] < 0.35$  gives the function

$$P(\text{planet}) = 0.29 + 0.51[\text{Si}/\text{Fe}]. \quad (21)$$

Therefore, although we predict a higher frequency of planets than observed, the slope of the planet-silicon correlation implied by our simulations reproduce the slope of planet-silicon correlation present in the SPOCS data, at least for metal-rich stars.



The difference between the empirical fit to the planet-silicon correlation in the above paragraph and that of §3 is whether the non-detections of planets at low values of  $[\text{Si}/\text{Fe}]$  are assumed to be significant. Examination of Figure 3 shows that the lowest  $\sim 0.1$  dex of the  $[\text{Si}/\text{Fe}]$  range in each  $[\text{Fe}/\text{H}]$  bin contains no observed planets. This influences our process of finding the power-law exponent that best describes the SPOCS planet-silicon correlation by making the percent of stars with planets resemble a step function in  $[\text{Si}/\text{Fe}]$ . As discussed in §3, any attempt to fit a power law to a step function will force the power law to assume a high exponent. When we consider only the range of  $[\text{Si}/\text{Fe}]$  values where planets have been found, the planet-silicon correlation in SPOCS assumes an approximately linear form with a modest slope.

The paucity of detected planets at low values of  $[\text{Si}/\text{Fe}]$ , which in §3 forces the observed planet-silicon correlation to appear steeper than we predict it should be, may, as in the case of the planet-metallicity correlation, reflect observational bias against long-period planets. The Jovian planets that form around  $\alpha$ -poor stars are, as in the case of iron-poor stars, most likely to finish forming too late to experience Type II migration. These planets are therefore less likely to be detected than the Jovian planets orbiting  $\alpha$ -rich stars.

#### 4.3.6. *Other Elements that may Correlate with Planet Frequency*

To the extent that titanium can be said to share properties of the pure  $\alpha$ -elements, the question of why planet hosts do not appear to be titanium enhanced is puzzling. If  $[\text{O}/\text{Fe}]$  does actually decline with increasing  $[\text{Fe}/\text{H}]$  in the range  $-0.8 < [\text{Fe}/\text{H}] < 0.5$ , then  $[\text{Ti}/\text{Fe}]$ , which exhibits the same declining trend in the SPOCS data, might actually be the best tracer of  $[\text{O}/\text{Fe}]$ —though other observers, including Soubiran & Girard (2005) and Bodaghee et al. (2003) have found that  $[\text{Ti}/\text{Fe}]$  as a function of  $[\text{Fe}/\text{H}]$  is flat for metal-rich stars. Since the assumed correlation between silicon and oxygen abundance is the basis for our prediction that silicon enhancement in planet hosts would result from planet formation by core accretion, we would expect planet hosts to be titanium-enhanced if  $[\text{Ti}/\text{Fe}]$  is the best tracer of  $[\text{O}/\text{Fe}]$ . Silicon, however, may not derive its predictive power of planet formation exclusively from a correlation with oxygen. At Jupiter’s position in a planet-forming disk of Solar composition, silicon is the third most abundant solid material at the ice line, after oxygen and iron. Even if a disk has low  $[\text{O}/\text{Fe}]$ , a high value of  $[\text{Si}/\text{Fe}]$  may give it enough solid material to form a planet. This is a property that titanium cannot share, as it is  $\sim 400$  times less abundant than silicon in solar-type stars.

Since we are assuming that  $[\text{Si}/\text{Fe}]$  is a proxy for  $[\alpha/\text{Fe}]$ , one test of our simulation results would be to replicate the analysis in §2 on other  $\alpha$ -elements. We predict that planet

hosts have enhanced abundances of C, Ne, Mg, S, Ar, S, and most especially O. We also suspect that enrichment is most likely to be observed in the subset of the  $\alpha$ -elements that, like silicon, are particularly important grain-forming materials: oxygen, carbon and magnesium. For example, as a noble gas, argon can have no direct influence on planet formation and would function only as an indicator of the presence of other core-forming materials. Though the fiducial  $[\text{Ar}/\text{Fe}]$  vs.  $[\text{Fe}/\text{H}]$  sequence follows the same general pattern as  $[\text{O}/\text{Fe}]$  vs.  $[\text{Fe}/\text{H}]$ , there is scatter in both these relations, so the Ar/O ratio changes somewhat among metal-rich stars. This scatter would lessen the utility of argon abundance as a predictor of planet formation. The diluting effect of scatter in Si/O on the planet-silicon correlation could be counteracted by the fact that silicon is an important core-forming material in its own right. Since our simulation assumes that Si/O is constant in all metal-rich stars, our prediction is that the planet-oxygen correlation has the same slope as the planet-silicon correlation, such that

$$P(\text{planet})_{\text{model}} = C + 0.51[\text{O}/\text{Fe}]. \quad (22)$$

Our simulation does not explore the effects of enhancing abundant non- $\alpha$  elements such as nickel. In the simplest interpretation of the core-accretion theory, where all solids are equally useful for forming planets, the planet-nickel correlation should be much weaker than the planet-silicon correlation, because of the low abundance of nickel compared with silicon and oxygen. Our statistical analysis indicates that  $[\text{Ni}/\text{Fe}]$  values are statistically enhanced for planet-bearing stars by a degree similar to that observed for silicon. If this result persists when more stars have been observed, it may indicate that not all solids are equally good for planet formation: some may accelerate or retard core growth through microchemical processes.

## 5. Conclusion

We find that there is statistical evidence for silicon and nickel enrichment of planet hosts in the SPOCS data of Valenti & Fischer (2005). Although the planet hosts do not exhibit any anomalous abundance patterns that indicate that they might be members of a different stellar population than other field stars, they do have values of  $[\text{Si}/\text{Fe}]$  and  $[\text{Ni}/\text{Fe}]$  that are systematically enhanced over other stars of the same  $[\text{Fe}/\text{H}]$ .

We have constructed Monte Carlo simulations that predict the likelihood of forming planets by core accretion in disks of differing mass, lifetime, outer radius and chemical composition. Our simulations reproduce both the planet-metallicity correlation and the planet-silicon correlation reported in this work. The simulation demonstrates that the abundance patterns of planet hosts in the SPOCS data are consistent with planets having formed by

core accretion. According to the core accretion theory, planets form most easily in ice-rich disks. We predict that the observed silicon enhancement of planet hosts arises primarily from the correlation in the abundances of silicon and oxygen, and secondarily from silicon’s own importance as a grain-forming material. The planet-silicon correlation would naturally arise if the core of Jupiter is made mainly of water ice frozen on silicate and/or iron grains. (See, however, Lodders (2004), which argues that Jupiter’s core may have formed from a tar-like mixture of organic compounds.)

More observations are needed to determine whether the planet-silicon correlation is robust, and whether it truly takes the form predicted by our simulations. Despite its large size, the SPOCS catalog is seriously affected by small-sample statistics when the planet hosts are separated into  $[\text{Fe}/\text{H}]$  bins to have their abundance patterns analyzed. The tantalizing suggestion that a silicon correlation may exist in the data underscores the need for a larger pool of stars from which to draw planet hosts and control sets. Our simulation predicts that the silicon effect should persist in a larger sample. Although we do not directly simulate variations in nickel abundance, the idea that nickel enhancement increases likelihood of planet formation is consistent with the core accretion theory. However, if all solids form protoplanetary cores equally well, the planet-silicon correlation should be much stronger than the planet-nickel correlation.

The most immediate test of our simulation is whether planet hosts show oxygen enhancement. Our simulation relies on the assumed correlation between oxygen and silicon abundances, so our analytical framework would be invalidated if a SPOCS-type survey shows no evidence for oxygen enrichment in planet hosts. Other  $\alpha$ -elements should also be correlated with the presence of planets, particularly the important core-forming materials C and Mg.

The question of what fraction of Pop I stars have at least one giant planet has been much debated recently. Our prediction of planetary systems around 16% of FGK dwarfs roughly agrees with the Marcy et al. (2005) extrapolation of the planet frequency-semimajor axis relation in the Lick/Keck/AAT planet search data. According to our calculation of the fraction of giant planets that experience Type II migration, planets on Jupiter-like orbits account for at least 4% of giant planet systems. A Solar system-like configuration of planets, while not particularly common, is nevertheless a viable outcome of the core accretion-migration scenario of planet formation. Detection of planets by transit searches and direct imaging will aid in solving the problem of completeness in discoveries of planets at 3-20 AU orbits, since these survey methods are sensitive to planets in a complementary part of the mass and semimajor axis parameter space to current Doppler surveys.

This work was supported by the National Science Foundation Graduate Research Fellow-

ship awarded to S. R., by the NASA Origins of Solar Systems program grant NNG04GN30G and a National Science Foundation Career Grant to G. L., and by NASA grant NAG-5-13285 and NSF grant AST-0507424 to P. B.

### A. Statistical Methods: Determining Significance of Planet-[Si/Fe] Correlation

We used the following procedure to find  $D_X$  and  $D_{\text{Fe}}$ :

1. Generate a bootstrap realization of SPOCS, a compilation of stellar abundances randomly selected from SPOCS. Choose stars at random from the SPOCS catalog to form set  $A$ , which will have the same number of members as the SPOCS catalog. Each star is selected independently of previously selected members of  $A$ , thus allowing duplicate entries in  $A$ .  $A$  will include both planet hosts and planetless stars in roughly the same proportions as in the SPOCS catalog. The set  $A$  is therefore a synthetic SPOCS compilation, created by sampling the SPOCS catalog with replacement.
2. Identify the planet hosts in  $A$ . These will comprise set  $B$ . The number of occurrences of each planet host in  $A$  is preserved in  $B$ , so where the same SPOCS planet host is present more than once in  $A$ , it will also be duplicated in  $B$ .
3. Find the iron-metallicity distribution of the planet hosts in the bootstrap realization of SPOCS by creating a normalized histogram of the [Fe/H] values of the stars in  $B$ . This is the [Fe/H] distribution of the planet hosts in the synthetic SPOCS catalog. Each iteration of this procedure will produce a slightly different planet-host [Fe/H] distribution, so our statistical analysis takes into account the fact that the planet hosts in SPOCS cannot be a perfect representation of the [Fe/H] distribution of all planet hosts in the Solar neighborhood.
4. Populate a control set  $C$ , with the same [Fe/H] distribution as  $B$  and including both planetless stars and planet hosts (simulating a collection of Pop I field stars selected independently of their planet status):
  - a Select a value of [Fe/H], from a uniform distribution that stretches between the minimum and maximum values of [Fe/H] in  $B$ .
  - b From a uniform distribution, select a probability of inclusion in the control set  $C$ .
  - c If the randomly selected probability of inclusion in  $C$  is less than or equal to the value of the normalized [Fe/H] histogram of  $B$  at the randomly selected value of [Fe/H], include in  $C$  the member of  $A$  with the metallicity nearest this value.

- d Repeat until the control set  $C$  has the same number of stars as the set of planet hosts  $B$ .
- 5. Use the K-S test to calculate  $k$ , the probability that  $B$  and  $C$  have the same underlying  $[X/Fe]$  distribution.
- 6. Use the K-S test to calculate  $q$ , the probability that  $B$  and  $C$  have the same underlying  $[Fe/H]$  distribution. Again,  $\mathcal{Q}$ , the distribution underlying  $q$ , is unity by construction. In practice,  $q$  will always be lower than 1, because of the impossibility of selecting two distinct sets of stars with exactly matching  $[Fe/H]$  distributions from a data set with a finite number of members.
- 7. Repeat until 100,000 Monte Carlo simulations have been performed, then find  $D_X$  and  $D_{Fe}$  by creating histograms of the values of  $k$  and  $q$  returned by each iteration. After 100,000 simulations,  $D_X$  and  $D_{Fe}$  become well populated, smooth distributions suitable for comparison.

## B. Statistical Methods: Determining Exponent $b$ of Planet-Silicon Abundance Power Law

We used the following procedure to find  $H$  for each value of  $b$ :

1. Generate a synthetic SPOCS compilation of stellar abundances  $A$ , with the same number of stars as SPOCS (1040), by sampling with replacement. (For details of sampling with replacement, see A.) Ignore any known planets: Stars in  $A$  will be assigned synthetic planets based on  $[Fe/H]$  and  $[Si/Fe]$ .
2. Select the value of  $b$ , the power-law exponent in equation 3, that you wish to test.
3. Calculate  $\mathcal{F}([Fe/H], [Si/Fe])$ , the probability that a planet will be found around a star of a given  $[Fe/H]$  and  $[Si/Fe]$ :
  - a Separate the stars in  $A$  into  $[Fe/H]$  bins,  $i$ , of width 0.1 dex. In each bin  $i$ , set  $\mathcal{F} = 0$  outside the minimum and maximum values of  $[Si/Fe]$ .
  - b Find the number of stars in  $i$ ,  $N_i$ , and calculate the value of the planet-metallicity correlation of equation 2 in each bin.
  - c Separate the stars in  $i$  into  $[Si/Fe]$  bins,  $j$ , of width 0.05 dex. Create a histogram of  $[Si/Fe]$  values in  $i$ ,  $h_j$ .

d Set the planet-silicon correlation such that

$$\mathcal{F}_{i,j} = C \times 10^{b[\text{Si/Fe}]_j}.$$

Find  $C$  such that the *average* of the nonzero values of  $\mathcal{F}$  in  $i$ , is equal to the value of the planet-metallicity correlation in  $i$ :

$$C_i = \frac{0.03 \times N_i 10^{2.0[\text{Fe/H}]_i}}{\sum_j h_j 10^{b[\text{Si/Fe}]_j}}.$$

4. Assign planets to the stars in  $A$ , to form the set of planet hosts  $B$ :
  - a From a uniform distribution, find a random deviate  $R$ , corresponding to the probability that the  $n^{\text{th}}$  star in  $A$ ,  $A_n$ , will have a planet.
  - b Find  $\mathcal{F}_n$ ,  $\mathcal{F}$  at the values of  $[\text{Fe/H}]$  and  $[\text{Si/Fe}]$  corresponding to  $A_n$ .
  - c If  $R \leq \mathcal{F}_n$ ,  $A_n$  is given a planet. If not,  $A_n$  will be planetless.
  - d Repeat for all stars in  $A$ . Although the particular stars that receive planets are different for each new set  $A$ , the overall fraction of stars with planets will always be  $\sim 6\%$ , as in SPOCS.
5. Find the iron-abundance distribution of the synthetic planet hosts: Calculate the normalized histogram of  $[\text{Fe/H}]$  for all stars in  $B$ .
6. Select a control set,  $C$ , with the same number of members and the same  $[\text{Fe/H}]$  distribution as  $B$ , making no reference to planet status:
  - a Select a value of  $[\text{Fe/H}]$ , from a uniform distribution with a spread equal to the range of  $[\text{Fe/H}]$  values present in  $B$ .
  - b Select a probability of inclusion in  $C$  from a uniform distribution.
  - c If the selected probability of inclusion in  $C$  is less than or equal to the normalized  $[\text{Fe/H}]$  histogram of  $B$  at the randomly selected value of  $[\text{Fe/H}]$ , include the star in  $A$  with  $[\text{Fe/H}]$  nearest this value in the control set  $C$ .
  - d Repeat until  $C$  has the same number of members as  $B$ .
7. Use the K-S test to calculate the probability,  $p$ , that  $B$  and  $C$  have the same underlying  $[\text{Si/Fe}]$  distribution.
8. Repeat for 10,000 Monte Carlo simulations, then find  $H$  by calculating the histogram of  $p$ . Compare  $H$  with  $D_{\text{Si}}$  to figure out whether the chosen value of  $b$  produces a planet-silicon correlation that matches what is observed in SPOCS.

## REFERENCES

- Adams, F. C., & Fatuzzo, M. 1996, *ApJ*, 464, 256
- Alcalá, J. M., Krautter, J., Covino, E., Neuhaeuser, R., Schmitt, J. H. M. M., & Wichmann, R. 1997, *A&A*, 319, 184
- Anders, E., & Grevesse, N. 1989, *Geochim Cosmochim. Acta*, 53, 197
- Andrews, S. M., & Williams, J. P. 2005, *ApJ*, 631, 1134
- Bodaghee, A., Santos, N. C., Israelian, G., & Mayor, M. 2003, *A&A*, 404, 715
- Boss, A. P. 2002, *ApJ*, 576, 462
- Briceño, C., et al. 2001, *Science*, 291, 93
- Calvet, N. 2003, *IAUS*, 219, 256
- D’Angelo, G., Kley, W., & Henning, T. 2003, *ApJ*, 586, 540
- D’Antona, F., Mazzitelli, I. 1994, *ApJS*, 90, 467
- Ecuivillon, A., Israelian, G., Santos, N. C., Mayor, M., Villar, V., & Bihain, G. 2004, *A&A*, 426, 619
- Eisner, J. A., & Carpenter, J. M. 2003, *ApJ*, 598, 1341
- Fischer, D. A., & Valenti, J. 2005, *ApJ*, 622, 1102
- Feltzing, S., & Gustafsson, B. 1998, *A&AS*, 129, 237
- Gonzalez, G. 1997, *MNRAS*, 285, 403
- Haisch, K. E., Lada, E. A., & Lada, C. J. 2000, *AJ*, 120, 1396
- Haisch, K. E., Lada, E. A., & Lada, C. J. 2001a, *AJ*, 121, 2065
- Haisch, K. E., Lada, E. A., & Lada, C. J. 2001b, *ApJ*, 553, L153
- Henry, L. G., Forbes, J. E., & Gould, N. L. 1964, *ApJ*, 139, 306
- Hersant, F., Gautier, D., & Lunine, J. I. 2004, *Planet. Space Sci.*, 52, 623
- Hollenbach, D., & Adams, F. C. 2004, in *ASP Conf. Ser. 323: Star Formation in the Interstellar Medium: In Honor of David Hollenbach*, 323, 3

- Huang, C., Zhao, G., Zhang, H. W., & Chen, Y. Q. 2005, *MNRAS*, 363, 71
- Hubickyj, O., Bodenheimer, P., & Lissauer, J. 2005, *Icarus*, in press
- Ida, S., & Lin, D. N. C. 2004a, *ApJ*, 604, 388
- Ida, S., & Lin, D. N. C. 2004b, *ApJ*, 616, 567
- Ida, S. & Lin, D. N. C. 2005, *ApJ*, 626, 1045
- Irvine, W. M., & Knacke, R. F. 1989, in *Origin and Evolution of Planetary and Satellite Atmospheres*, ed. S. K. Atreya, J. B. Pollack, & M. S. Matthews (Tucson: University of Arizona Press), 3
- Israelian, G., Santos, N. C., Mayor, M., & Rebolo, R. 2003, *A&A*, 405, 753
- Johnstone, D., Hollenbach, D., & Bally, J. 1998, *ApJ*, 499, 758
- Kenyon, S. J., & Gómez, M. 2001, *AJ*, 121, 2673
- Kenyon, S. J., & Hartmann, L. 1995, *ApJS*, 101, 117
- Kornet, K., Bodenheimer, P., Rózycka, M., & Stepinski, T. F. 2005, *A&A*, 430, 1133
- Laughlin, G. P., & Adams, F. C. 1997, *ApJ*, 491, 51L
- Laughlin, G., Bodenheimer, P., & Adams, F. C. 2004, *ApJ*, 612, 73
- Laughlin, G., & Rózycka, M. 1996, *ApJ*, 456, 279
- Lawson, W. A., Lyo, A.-R., & Feigelson, E. D. 2003, *IAY Symposium*, 219
- Lewis, J. S., & Prinn, R. G. 1980, *ApJ*, 238, 357
- Lodders, K. 2004, *ApJ*, 611, 587
- Marcy, G., Butler, R. P., Fischer, D., Vogt, S., Wright, J., Tinney, C. G., & Jones, H. R. A. 2005, *Progress of Theoretical Physics Supplement*, 158, 24
- McCaughrean, M. J., & O'Dell, C. R. 1996, *AJ*, 111, 1977
- Morbidelli, A., Crida, A., & Masset, F. 2005, *AAS/Division for Planetary Sciences Meeting Abstracts*, 37
- Murray, N., & Chaboyer, B. 2002, *ApJ*, 566, 442



- Nelson, R. P., Papaloizou, J. C. B., Masset, F., & Kley, W. 2000, MNRAS, 318, 18
- Nissen, P. E., & Edvardsson, B. 1992, A&A, 261, 255
- Osterloh, M., & Beckwith, S. V. W. 1995, ApJ, 439, 288
- Pasek, M. A., Milsom, J. A., Ciesla, F. J., Lauretta, D. S., Sharp, C. M., & Lunine, J. I. 2005, Icarus, 175, 1
- Papaloizou, J. C. B., & Nelson, R. P. 2005, A&A, 433, 247
- Papaloizou, J. C. B., & Terquem, C. 1999, ApJ, 521, 823
- Podolak, M. 2003, Icarus, 165, 428
- Pollack, J. B., Hubickyj, O., Bodenheimer, P., Lissauer, J. J., Podolak, M., & Greenzweig, Y. 1996, Icarus, 124, 62
- Prantzos, N., & Aubert, O. 1995, A&A, 302, 69
- Press, W. H., et al. 1992, Numerical Recipes in Fortran: The Art of Scientific Computing (Cambridge: Cambridge Univ. Press)
- Rice, W. K. M., Lodato, G., & Armitage, P. J. 2005, ArXiv Astrophysics e-prints, arXiv:astro-ph/0509413
- Sandquist, E., Taam, R. E., Lin, D. N. C., & Burkert, A. 1998, ApJ, 506, 65L
- Santos, N. C., Israelian, G., García López, R. J., Mayor, M., Rebolo, R., Randich, S., Ecuivillon, A., Domínguez Cerdeña, C. 2004, A&A, 427, 1085
- Schneider, G., Wood, K., Silverstone, M. D., Hines, D. C., Koerner, D. W., Whitney, B. A., Bjorkman, J. E., & Lowrance, P. J. 2003, ApJ, 125, 1467
- Shu, F. H., Najita, J., Ostriker, E. C., & Shang, H. 1995, ApJ, 455, 155
- Shu, F. H., Tremaine, S., Adams, F. C., & Ruden, S. P. 1990, ApJ, 358, 495
- Smith, V. V., Cunha, K., & Lazzaro, D. 2001, AJ, 121, 3207
- Sohl, F., Spohn, T., Breuer, D., & Nagel, K. 2002, Icarus, 157, 104
- Soubiran, C., & Girard, P. 2005, A&A, 438, 139
- Takeda, Y., & Honda, S. 2005, PASJ, 57, 65

- Takeuchi, T., Clarke, C. J., & Lin, D. N. C. 2005, *ApJ*, 627, 286
- Timmes, F. X., Woosley, S. E., & Weaver, Thomas A. 1995, *ApJS*, 98, 617
- Valenti, J. A. & Fischer, D. A. 2005, *ApJS*, 159, 141
- Vicente, S. M., & Alves, J. 2005, *A&A*, 441, 195
- Weidenschilling, S. J. 1977, *Ap&SS*, 51, 153
- Weinberger, A. J., Becklin, E. E., Schneider, G., Chiang, E. I., Lowrance, P. J., Silverstone, M., Zuckerman, B., Hines, D. C., & Smith, B. A. 2002, *ApJ*, 566, 409
- Weintraub, D. A., Saumon, D., Kastner, J. H., Forveille, T. 2000, *ApJ*, 530, 867

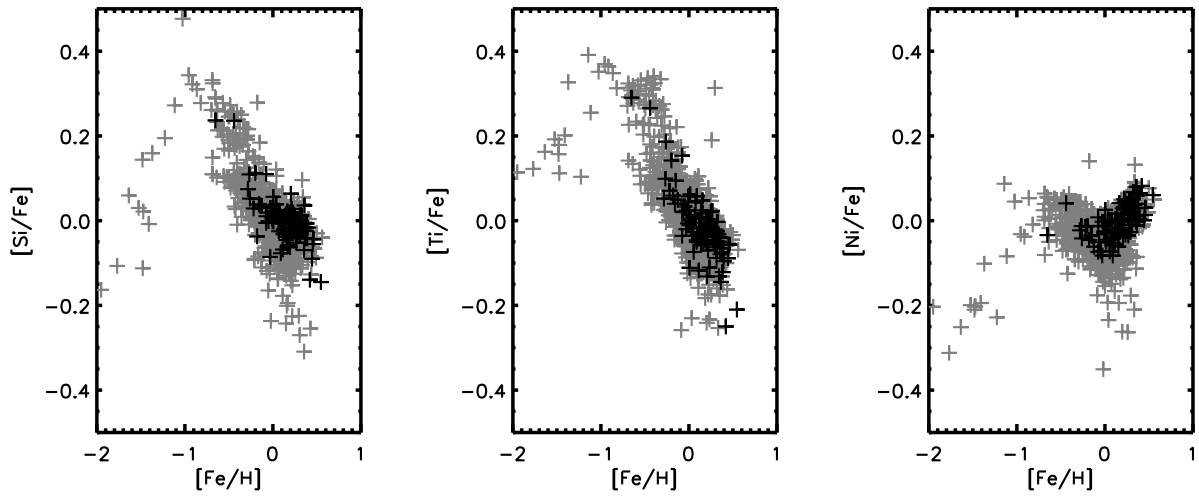


Fig. 1.—  $[\text{Si}/\text{Fe}]$  (left),  $[\text{Ti}/\text{Fe}]$  (middle), and  $[\text{Ni}/\text{Fe}]$  (right) as a function of  $[\text{Fe}/\text{H}]$  for the stars in the SPOCS data set. Known planet hosts are plotted in black and stars with no detected planetary companion are plotted in gray.

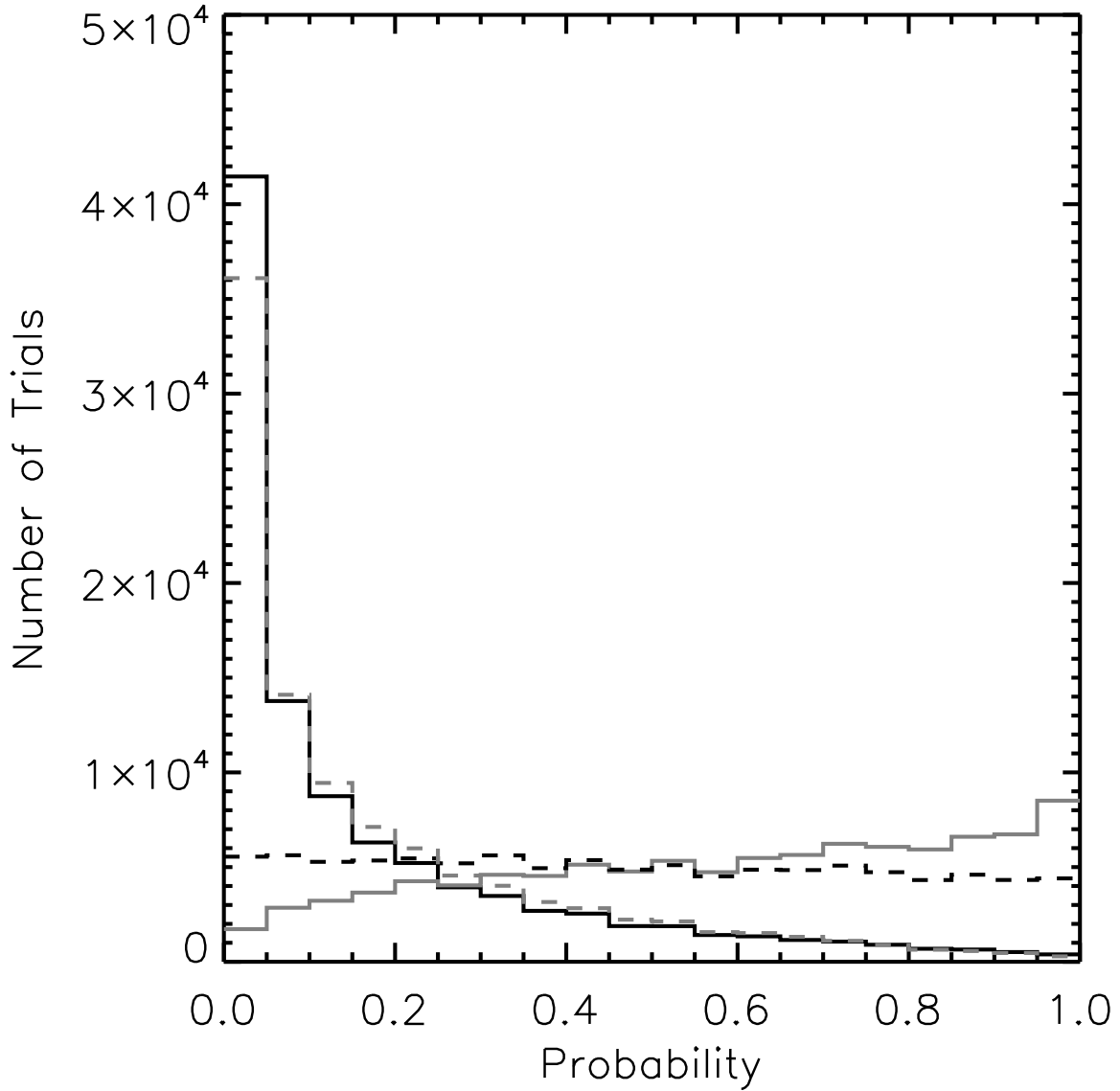


Fig. 2.— Histogram of probabilities, returned by the K-S test, that the planet hosts are from the same abundance distribution as the control set of field stars. The test results for [Si/Fe] are plotted in solid black, [Ti/Fe] in dash-dot black, [Ni/Fe] in dash-dot gray, and [Fe/H] in solid gray.

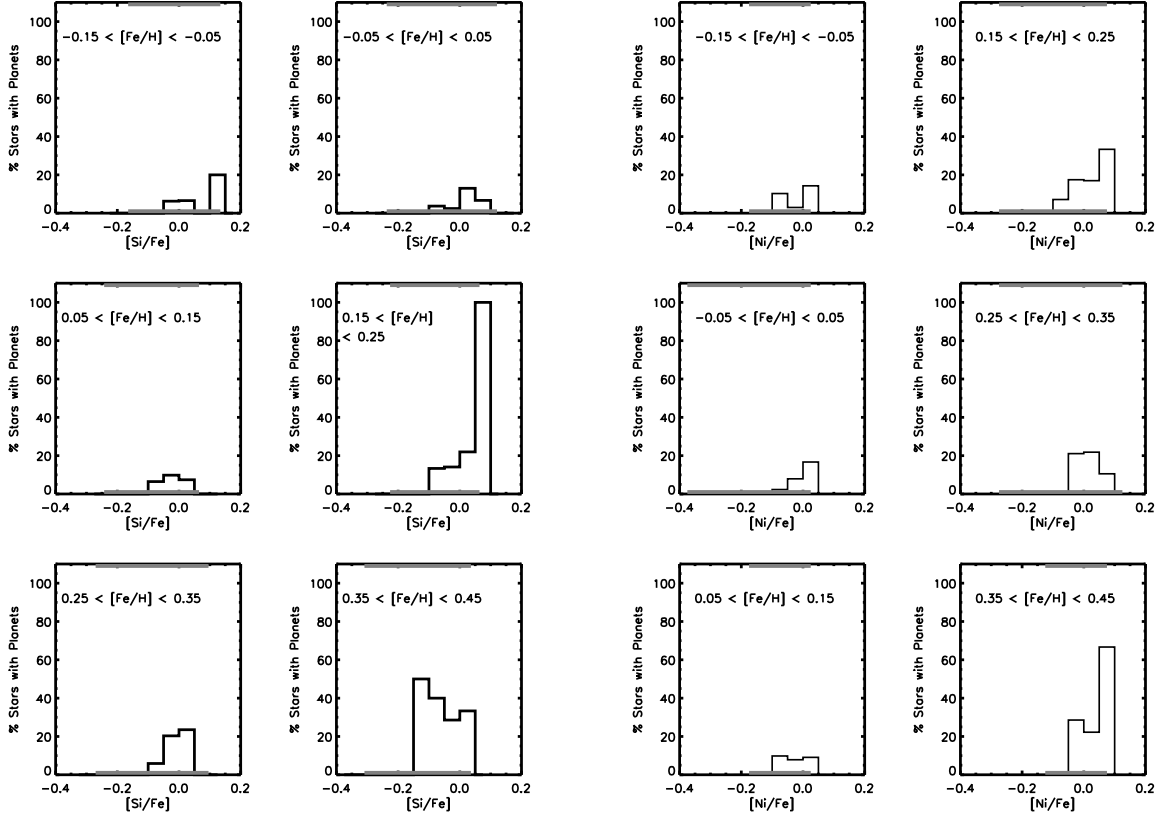


Fig. 3.— Percent of stars with planets as a function of  $[\text{Si}/\text{Fe}]$  (left) and  $[\text{Ni}/\text{Fe}]$  (right) for different bins in  $[\text{Fe}/\text{H}]$ . The gray bars on the bottom and top of the plot box show the range of values of  $[\text{X}/\text{Fe}]$  present in SPOCS in each individual  $[\text{Fe}/\text{H}]$  bin. Stars with planets always come from the top of the field-star  $[\text{Si}/\text{Fe}]$  and  $[\text{Ni}/\text{Fe}]$  ranges.

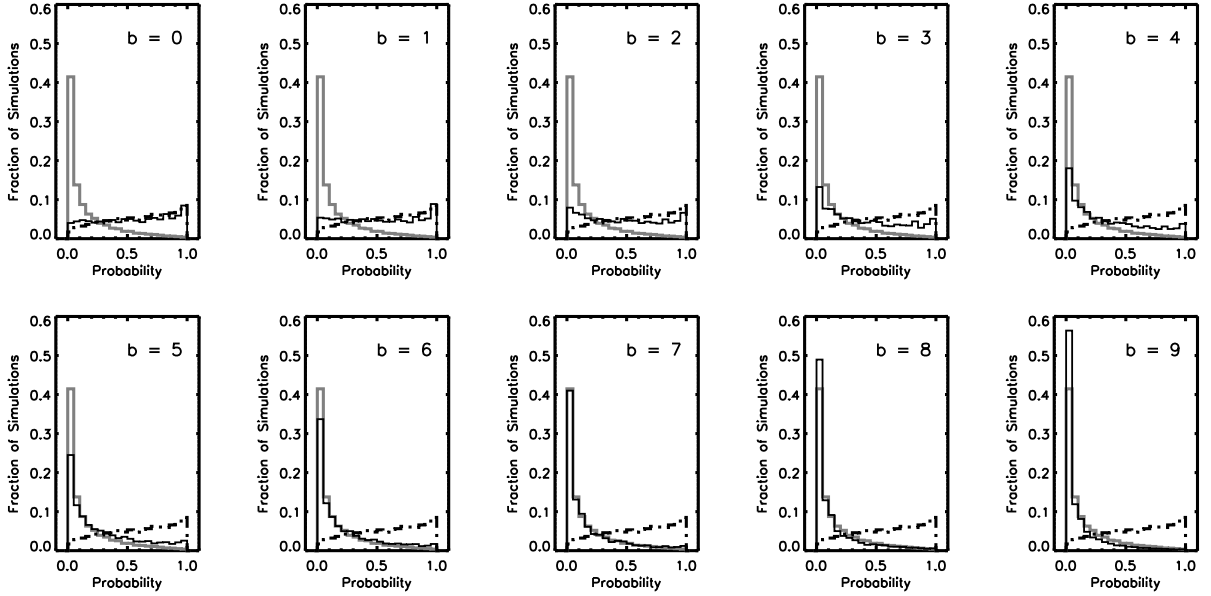


Fig. 4.— Results of simulations to determine power-law exponent governing the planet-silicon relation. In solid black are histograms of probability that planet hosts are drawn from the same silicon-abundance distribution as the field stars of the same iron abundances, if planet frequency follows a power law with exponent  $b$ . In each panel, the distribution  $D_{\text{Si}}$ , the probability that the actual planet hosts in SPOCS have the same silicon-abundance pattern as the field-star population, is shown in solid gray. For reference,  $D_{\text{Fe}}$ , the histogram of probabilities that sets of stars selected by iron abundance do, in fact, have matching  $[\text{Fe}/\text{H}]$  distributions, is plotted in dash-dotted black.

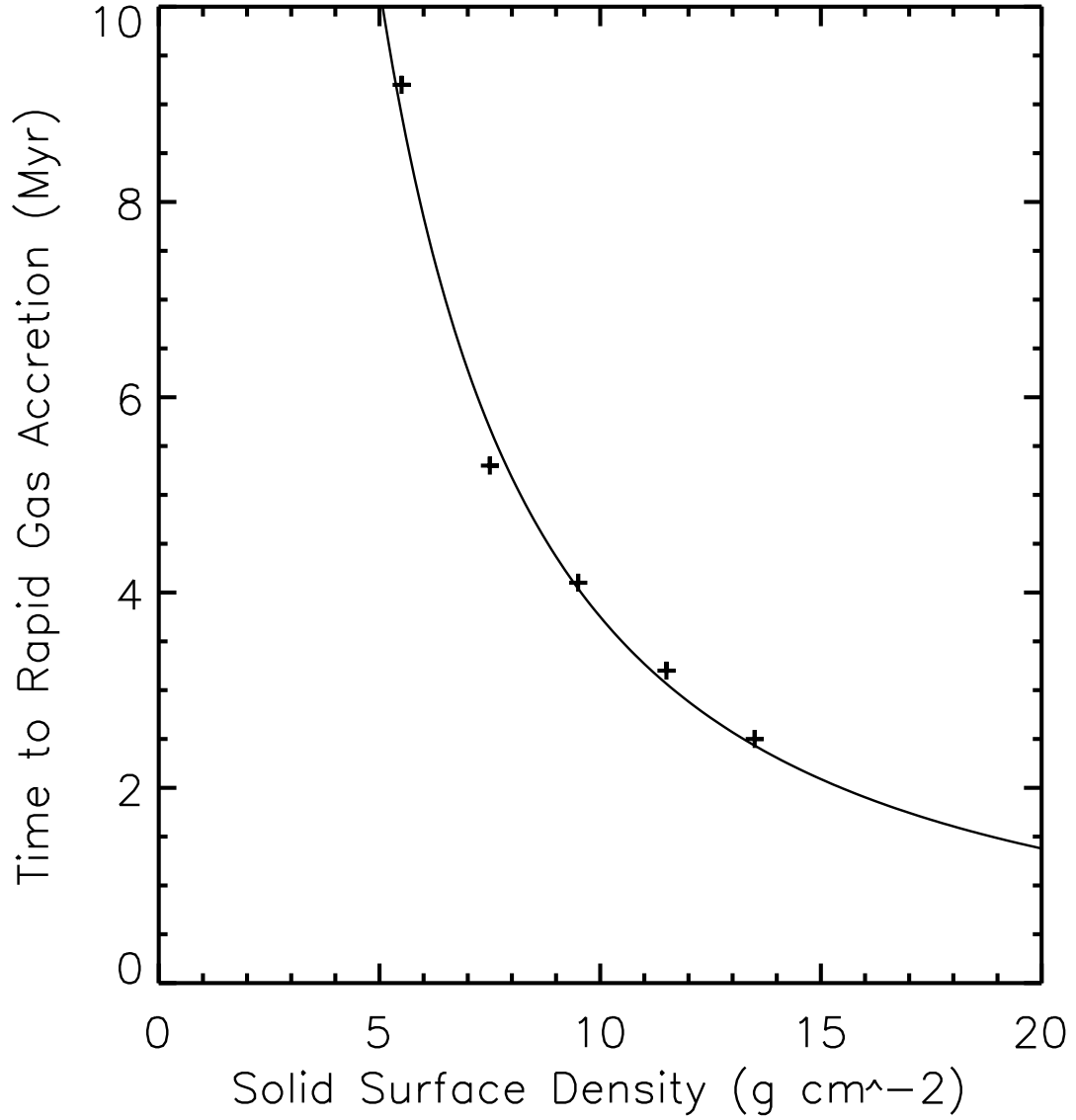


Fig. 5.— Time till gas accretion of a Jovian protoplanet, as a function of solid surface density, at 5.2 AU from the young Sun. A power law,  $t_{\text{rga}}(\sigma)$ , is plotted over points showing the results of five simulations.

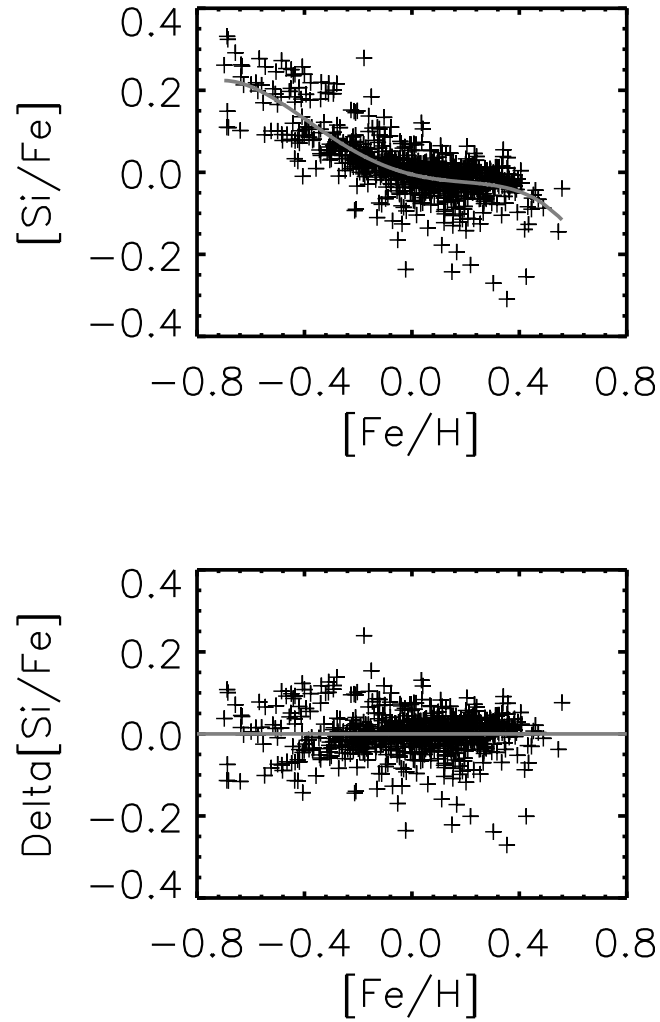


Fig. 6.— Top: Empirical model of  $[\text{Si}/\text{Fe}]$  as a function of  $[\text{Fe}/\text{H}]$ . + signs represent the SPOCS data; the gray, solid line is a fitted fourth-order polynomial. Bottom: Fit residuals. There is a slight trend toward increasing  $\Delta[\text{Si}/\text{Fe}]$  where  $[\text{Fe}/\text{H}] < -0.3$ , but for the most part the fit residuals are independent of  $[\text{Fe}/\text{H}]$ .



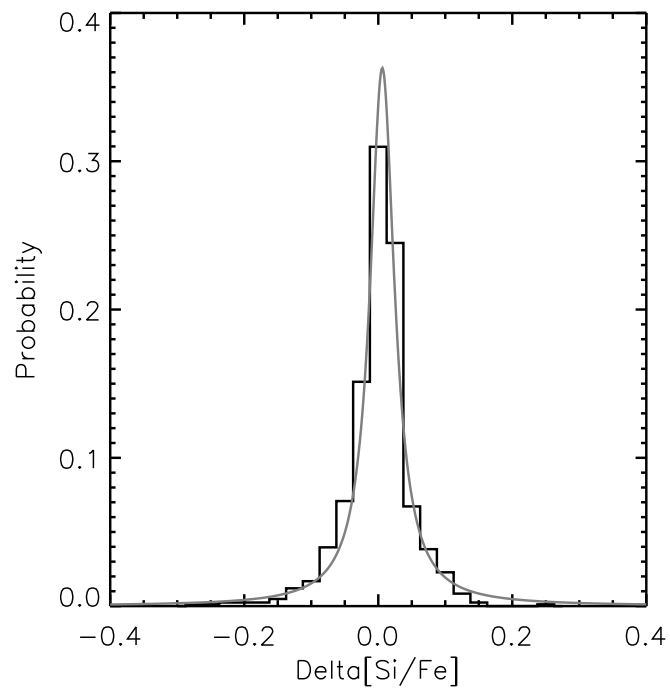


Fig. 7.— Model of residuals around fiducial  $[\text{Si}/\text{Fe}]([\text{Fe}/\text{H}])$ .  $\Delta[\text{Si}/\text{Fe}]$  is best characterized by a Cauchy distribution, which is used in our simulation to randomly select the deviation in  $[\alpha/\text{Fe}]$  from the fiducial for each star-disk system.

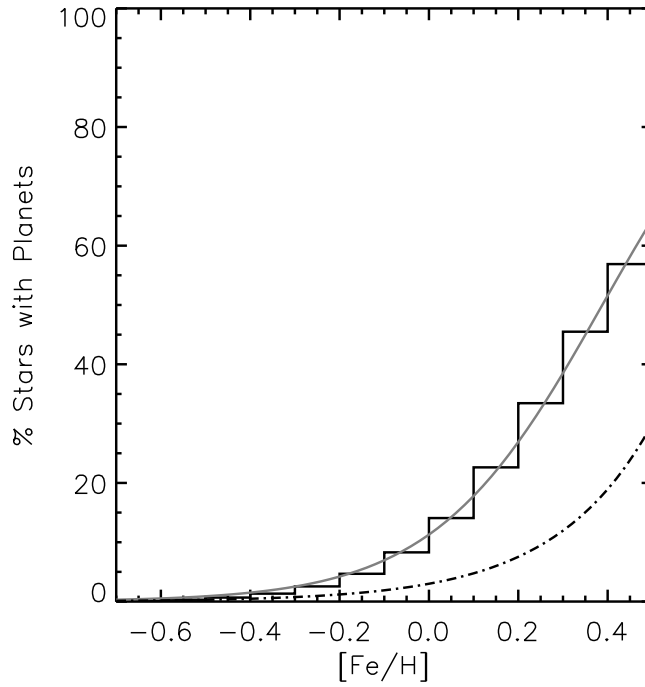


Fig. 8.— Planet-metallicity correlation as predicted by Monte Carlo simulations. The stair-stepped black line is a histogram showing the percent of stars with planets in each metallicity bin, as predicted by our simulations. Overplotted in smooth gray is our fit of a logistic function to the analytical planet-metallicity correlation. The dotted line is the planet-metallicity correlation measured by Fischer & Valenti (2005).

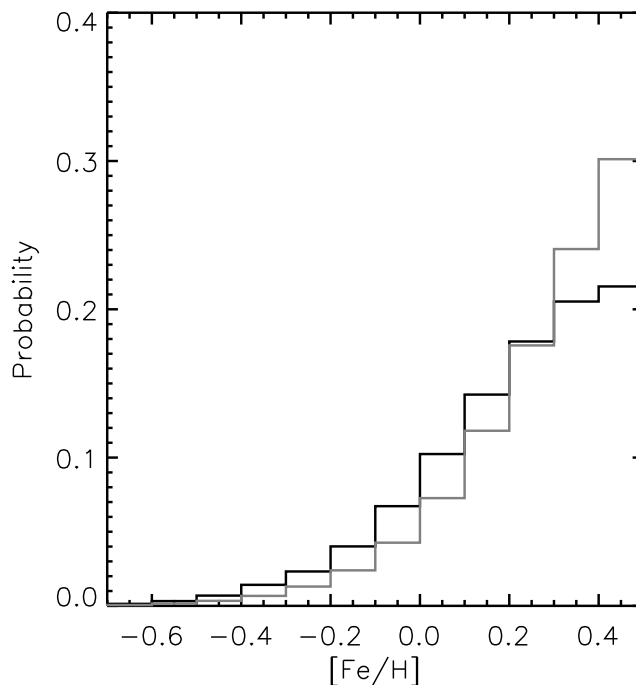


Fig. 9.—  $[\text{Fe}/\text{H}]$  distribution of hosts of long-period (black) and short-period (gray) planets in our simulation results. Hosts of short-period planets tend to be more metal-rich than hosts of long-period planets.



Fig. 10.— Left: Percent of stars with planets as a function of initial disk mass. Right: Percent of stars with planets as a function of disk lifetime. Our core accretion simulations indicate that the Solar nebula lasted for 5.2 Myr, at which 27% of stars form planets.

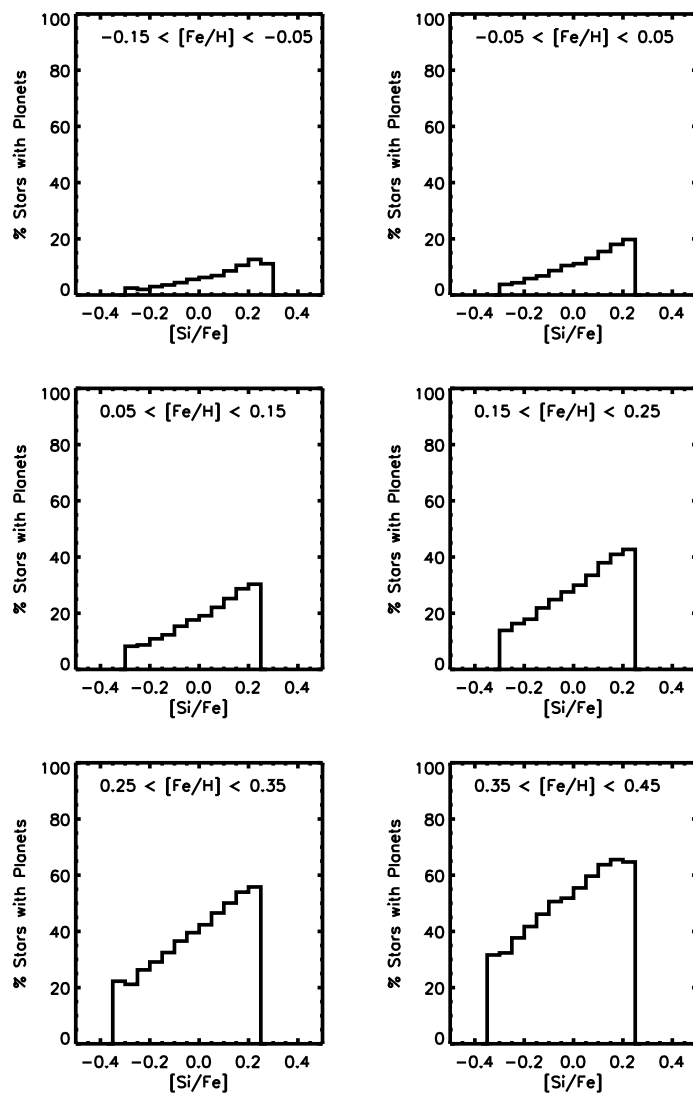


Fig. 11.— Percent of stars with planets as a function of  $[\text{Si}/\text{Fe}]$  at constant  $[\text{Fe}/\text{H}]$ , predicted by simulations. We model the fraction of stars with planets is a linear function of  $[\text{Si}/\text{Fe}]$  with a slope increasing with  $[\text{Fe}/\text{H}]$ .

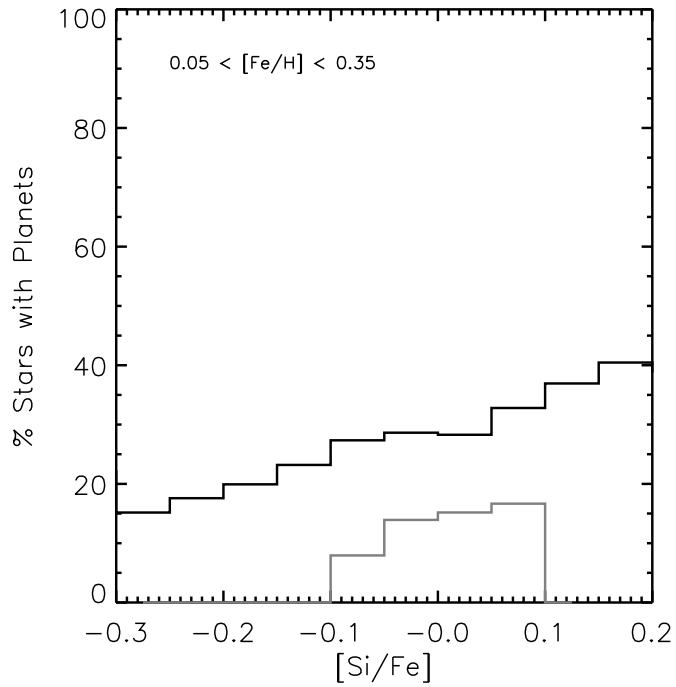


Fig. 12.— Comparison between theoretical (black) and observed (gray) percent of stars with planets, as a function of  $[\text{Si}/\text{Fe}]$ , for  $0.05 < [\text{Fe}/\text{H}] < 0.35$ . For stars in this  $[\text{Fe}/\text{H}]$  range, our simulations predict that the percent of stars with planets is a linear function of  $[\text{Si}/\text{Fe}]$  with a slope of 0.51. In the  $[\text{Si}/\text{Fe}]$  bins where the number of planets in SPOCS is nonzero, the slope of the observed planet-silicon correlation is 0.54.